Natural Resources Canada
Ressources naturelles Canada

GEOLOGICAL SURVEY OF CANADA
OPEN FILE 8240

Indicator mineral signature of the Strange Lake rare earth element deposit, Quebec and Newfoundland and Labrador

M.B. McClenaghan, R.C. Paulen, I.M. Kjarsgaard, S.A. Averill, and R. Fortin

2017

Celebrating 175 yrs

Canada

GEOLOGICAL SURVEY OF CANADA
OPEN FILE 8240

Indicator mineral signature of the Strange Lake rare earth element deposit, Quebec and Newfoundland and Labrador

M.B. McClenaghan[1], R.C. Paulen[1], I.M. Kjarsgaard[2], S.A. Averill[3], and R. Fortin[1]

[1]Geological Survey of Canada, Ottawa, Ontario
[2]Mineralogical Consultant, Ottawa, Ontario
[3]Overburden Drilling Management Ltd., Ottawa, Ontario

2017

https://doi.org/10.4095/306239

This publication is available for free download through GEOSCAN (http://geoscan.nrcan.gc.ca/)

Recommended citation
McClenaghan, M.B., Paulen, R.C., Kjarsgaard, I.M., Averill, S.A., and Fortin, R., 2017. Indicator mineral signature of the Strange Lake rare earth element deposit, Quebec and Newfoundland and Labrador; Geological Survey of Canada, Open File 8240, 1 zip file. https://doi.org/10.4095/306239

TABLE OF CONTENTS

Figures

Tables

Indicator mineral signature of the Strange Lake rare earth element deposit, Quebec and Newfoundland and Labrador

M.B. McClenaghan[1], R.C. Paulen[1], I.M. Kjarsgaard[2], S.A. Averill[3],and R. Fortin[1]

[1]Geological Survey of Canada, 601 Booth Street, Ottawa, Ontario K1A 0E8
[2]Mineralogical Consultant, 15 Scotia Place, Ottawa, Ontario K1S 0W2
[3]Overburden Drilling Management Limited, 107-15 Capella Court, Ottawa, Ontario K2E 7X1

ABSTRACT

The first detailed study of the indicator mineral signature of a major rare earth element (REE) deposit in glaciated terrain was undertaken at the Strange Lake Zr-Y-HREE deposit in northern Quebec and Newfoundland and Labrador, Canada. The heavy mineral (>3.2 SG) and mid-density (3.0–3.2 SG) non-ferromagnetic fractions of bedrock samples from the two mineralized zones were examined to determine potential indicator minerals of REE mineralization. Till samples overlying and up to 50 km down-ice of the deposit were examined to determine the abundance of these minerals at varying distances from the deposit. The deposit contains numerous oxide, silicate, phosphate, and carbonate indicator minerals. Some of the minerals observed in both the bedrock and till samples had not been previously reported for the Strange Lake deposit. The most useful indicator minerals were determined to be Zr-silicates (primary elpidite, secondary gittinsite, and many other hydrated Zr±Y±Ca-silicate minerals), pyrochlore, thorite/thorianite, monazite/rhabdophane, chevkinite, parisite, bastnaesite, kainosite, and allanite. Rare earth element indicator minerals can now be added to the expanding list of indicator minerals that can be used to explore for a broad range of deposit types and commodities, i.e., diamonds, precious metals, base metals, and strategic metals.

INTRODUCTION

Rare Earth Elements (REE) are used in a variety of products, including consumer electronics, green technology, and military defence systems (Hatch, 2012). Due to growing demand coupled with supply challenges related to China controlling the market (Verplanck and Van Gosen, 2011; Chakhmouradian and Wall, 2012; Hatch, 2012; Simandl et al., 2012; Simandl, 2014), there has been increased interest in exploration for REE in Canada. Although no REEs are currently being mined or processed in Canada, significant resource potential exists. Rare earth elements are hosted in peralkaline intrusions, carbonatite, pegmatite, and peraluminous granite (Mackay and Simandl, 2015; Simandl et al., 2015). Due to Canada's glaciated landscape, till geochemical and indicator mineral methods have the potential to be useful exploration tools.

The undeveloped Strange Lake peralkaline complex in eastern Canada contains one of the world's largest deposits of Zr, Y, and heavy rare earth elements (HREE) (Zajac, 2015). The deposit was sampled by the Geological Survey of Canada to test and demonstrate modern indicator mineral methods for detecting REE deposits using glacial sediments. This site was chosen because (1) the bedrock and surficial geology are well known and (2) there is a well documented radioactive boulder and REE-rich till dispersal train down-ice of the deposit.

This study was carried out as part of the Geological Survey of Canada's (GSC) Geo-mapping for Energy and Minerals (GEM) Program, Phase 2 (2013–2021), a federal geoscience program conducted in collaboration with the provinces and territories with a mandate to provide new regional geoscience data to support natural resource exploration in Northern Canada. Program activities include surficial and bedrock mapping, till geochemistry and indicator mineralogy studies, lake sediment geochemical surveys, and gamma-ray spectrometry studies in the Hudson-Ungava region (McClenaghan et al., 2014, 2015a). This report provides an overview of the mineralogical signatures in till around the Strange Lake deposit.

Location and access

The Strange Lake deposit is in eastern Canada, on the border between the provinces of Quebec and Newfoundland and Labrador (Fig. 1), centred on latitude 56°18 N and longitude 64°07'W in National Topographic System (NTS) map 24A/08. The deposit is southeast of Lac Brisson, approximately 240 km northeast of the town of Schefferville and 125 km west of the world-class Voisey's Bay Ni-Cu-Co mine in Labrador. The area is north of the tree line, in the zone of discontinuous permafrost, and is accessible only by air. A large lake 15 km to the northwest of the deposit was informally named Strange Lake by the geologists who discovered the deposit because of the "strange" minerals it contained (S. Zajac, pers. comm., 2016).

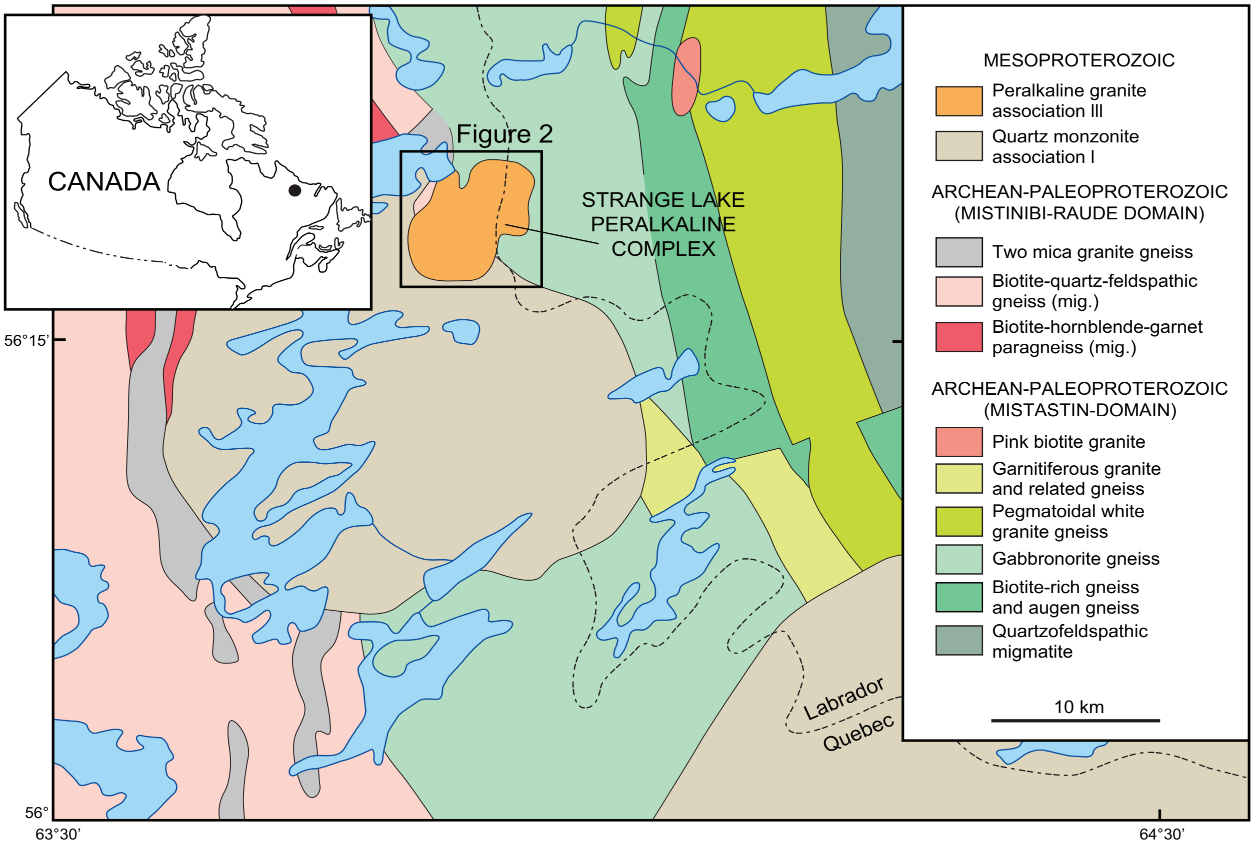

Figure 1. Location of the study area in eastern Canada (inset) and regional bedrock geology map of the Strange Lake area (modified from Miller et al., 1997).

GEOLOGY

Bedrock geology

The bedrock geology of the area is summarized below from Miller (1986, 1988, 1990, 1996), Sinclair et al. (1992), Kerr (2013), and Gowans et al. (2014). The Strange Lake intrusion is within the Paleoproterozoic Churchill Structural Province in the northeastern part of the Canadian Shield. The peralkaline granite, dated at 1240 +/- 2 Ma (Miller, 1990), intrudes along the contact between Late Archean to Early Proterozoic metasedimentary and metagabbroic rocks to the north and Middle Proterozoic quartz monzonite to the south (Fig. 1). The complex, approximately 7 km in diameter, consists of at least three varieties of peralkaline granite. The complex has been divided into four granitic subunits by Miller (1986, 1990) based on the mineralogy and presence of inclusions (Fig. 2). The highest grade mineralization is in pegmatite-aplite dykes that are associated with the exotic-rich granite in the central part of the intrusion (Main Zone) and the northwest edge (B Zone) (Fig. 2).

The Strange Lake intrusion comprises many rare minerals containing incompatible elements that, at the time of the intrusion's discovery, were unnamed. A list of potential indicator minerals contained in the deposit and the elements they host are summarized from Jambor et al. (1996, 1998), Birkett et al. (1992, 1996), Miller et al. (1997), and Zajac (2015) in Table 1. The deposit is relatively enriched in heavy REE (Eu to Lu) and Y compared to light rare earth elements (LREE). Most REE in the deposit are hosted by the minerals gerenite, kainosite, and gadolinite. Zirconium is hosted mainly by gittinsite, elpidite, armstrongite, and minor zircon. Thorite hosts most of the Th, and Nb is hosted mainly by pyrochlore. The principle hosts of Y are gerenite-(Y) and kainosite-(Y). The main source of Be in the deposit is the gadolinite-group minerals.

Discovery of the Strange Lake deposit

The Strange Lake intrusion was discovered by the Iron Ore Company of Canada in 1979 in a follow-up of a lake sediment anomaly first reported by the Canada-Newfoundland Uranium Reconnaissance Program (Hornbrook et al., 1979; McConnell and Batterson, 1987; Zajac, 2015). Hornbrook et al.'s (1979) reconnaissance-scale lake sediment and water data revealed anomalies for Pb and Zn in lake sediments and U and F in lake water that extended between 25 and 40 km down-ice (northeast) from what was later discovered to be the mineralized intrusion. From 1980 to 2006, several companies explored the property and two mineralized zones were identified, the Main Zone (formerly the A Zone) and the B Zone (Fig. 2). The B Zone is the

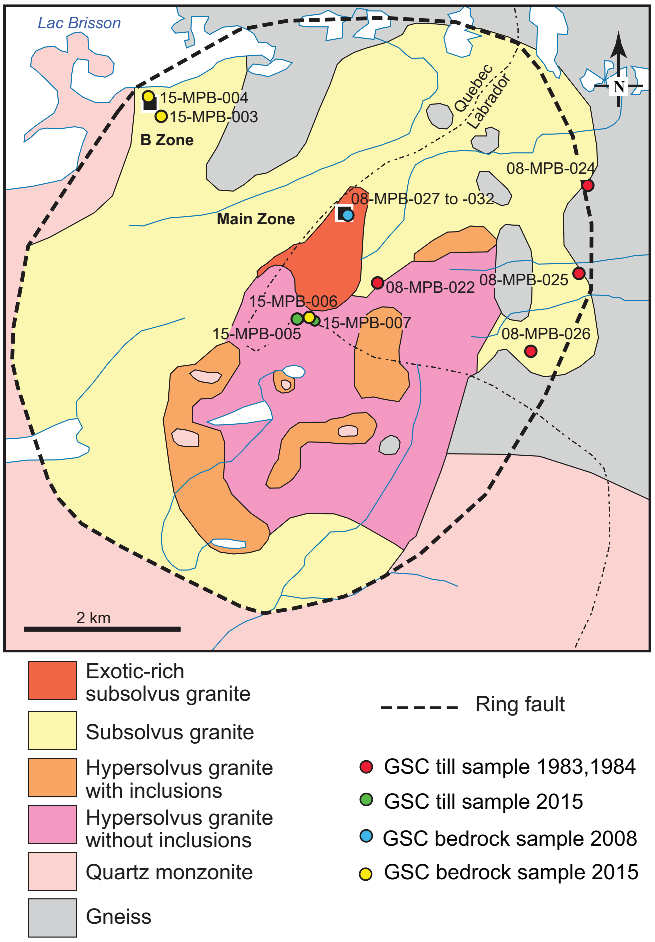

Figure 2. Simplified bedrock geology map of the Strange Lake intrusion, modified from Kerr (2013), after Miller (1986) and Miller et al. (1997). The Main and B zones are shown.

largest resource with indicated mineral resources of 278 Mt at 0.93% total rare earth element oxide (TREO) and inferred mineral resources of 214 Mt at 0.85% TREO (Gowans et al., 2014). The resource for the smaller Main Zone has been estimated at 55.8 Mt with a grade of 2.99% ZrO_2, 0.38% Y_2O_3, 0.29% Nb_2O_5, 0.08% BeO (Kerr and Rafuse, 2012; Kerr, 2013).

Gamma-ray signature

The Strange Lake intrusion has a strong gamma-ray signature that was identified in the 1980s by the Geological Survey of Canada. Cumulative values for eTh (Fig. 3) and eU reflect the presence of the intrusion as well as radioactive boulders and minerals in till that have been dispersed at least 50 km down-ice to the east-northeast (Zajac, 2015). The upper half of the Main Zone has been removed through erosion, which Zajac (2015) attributed to glaciation. The Strange Lake intrusion is highly altered, making it likely that regolith was formed by preglacial preferential weathering of the upper part of the intrusion as compared to the surrounding bedrock. This Main Zone regolith was likely the source for the significant volume of REE-rich debris that was glacially eroded and dispersed over the long distances (at least 50 km) in a single and narrow east-northeast-trending ribbon (Batterson and Taylor, 2009), likely by a paleo ice stream (Paulen et al., 2017). In contrast, the B Zone underwent only minimal glacial erosion and is largely intact. Due to its grade and tonnage, the B Zone has the potential for future development (Gowans et al., 2014).

Surficial geology

The Strange Lake deposit was strongly scoured by the Laurentide Ice Sheet, from an ice dome that developed during the Wisconsin, west of the George River in Quebec (Dyke and Prest, 1987a). Ice flowed eastward over Strange Lake during all phases of the Wisconsinan glaciation, as the Ancestral Labrador divide migrated to the George River basin, but remained west of Strange Lake (Vincent, 1989).

The surficial geology of the region (Fig. 4) was mapped by Batterson (1989) and Batterson and Taylor (2005a,b). The study area is covered by a till blanket of varying thickness, ranging from a veneer (<2 m) to several metres with rare interspersed bedrock outcrops There are thin (<1 m) organic deposits in low-lying areas. Examination of satellite imagery and digital elevation models (DEM) of the Lac Brisson and Strange Lake area provide evidence that the landscape was impacted by fast glacial flow (i.e. an ice stream) (Fig. 5). Large groups of elongated streamlined forms (mega-flutings, mega-lineations, crag- and-tail forms) are juxtaposed with areas devoid of such features, suggesting relatively fast and slow paleo ice flow, respectively. Mega-scale glacial lineations have been identified from various types of imagery, as well as during fieldwork, and are most commonly expressed as clusters of glacial lineations with length-to-width ratios that exceed 12 (Paulen et al., 2017). Margold et al. (2015) identified the Kogaluk River ice stream (IS #187) that flowed across the study area and placed the Strange Lake REE deposit directly within it's trunk. Measurements of striae and landforms indicate that the ice stream flowed to the Labrador coastline in an east-northeast trajectory (Fig. 5).

After the ice-stream glacial land system shut down, the region was affected by a localized glacial land-system with ice-flow controlled by topography, as the retreating Laurentide Ice Sheet was directed into a number of fjords that dissect the Nain plateau. At Strange Lake, ice was directed to the northeast toward Anaktalik Brook and Tasisuak Lake, which imparted light striae on the outcrops, but did not rework the mega-scale glacial lineations formed by the ice stream and, more importantly, did not rework the Strange Lake dispersal train. During this retreat phase, east-north-east-trending meltwater corridors deposited ice-contact

Table 1. List of potential indicator minerals in the Strange Lake deposit compiled from Birkett et al. (1992), Miller (1996), Jambor et al. (1998), and Gowans et al. (2014). Indicator minerals that were recovered from bedrock and till samples in this study are indicated.

Mineral	Formula	Hardness*	Density*	Reported by others	Seen in bedrock PTS in this study	Seen in bedrock HMC in this study	Seen in till HMC in this study	Element source in glacial dispersal train
U, Th minerals								
cerianite	$(Ce,Th)O_2$	not determined	7.2	no	no	yes	no	Ce, Th
thorite	$Th(SiO_4)$	5.0	4–6.7	Miller (1996)	no	yes	yes	Th
thorianite	ThO_2	6.0	10.0	no	yes	yes	yes	Th
uraninite	UO_2	5–6	6.5–10.95	no	yes	yes	no	U
Zr minerals								
elpidite	$Na_2ZrSi_6O_{15}•3(H_2O)$	7	2.54	Birkett et al. (1992)	yes	no	yes	Zr
hilairite	$Na_2ZrSiO_3O_9•3H_2O$	4.5	2.72	Roelofson and Veblen (1999)	no	no	no	Zr
dalyite	$K_2ZrSi_6O_{15}$	7.5	2.84	Birkett et al. (1992)	no	no	no	Zr
vlasovite	$Na_2ZrSi_4O_{11}$	6	2.97	Birkett et al. (1992)	no	no	no	Zr
zircon	$ZrSiO_4$	7.5	4.6–4.7	Birkett et al. (1992)	yes	yes	yes	Zr
armstrongite	$CaZrSi_6O_{15}•3(H_2O)$	4.5	2.7	Birkett et al. (1992)	no	no	no	Zr
catapleiite	$NaZrS_33O_9•2(H_2O)$	4.5–5	2.8	Birkett et al. (1992)	yes	yes	no	Zr
Ca-catapleiite	$CaZrSi_3O_9•2(H_2O)$	4.5–5	2.8	Birkett et al. (1992)	yes	yes	no	Zr
calciohilairite	$CaZrSi_3O_9•3(H_2O)$	4	2.68	Birkett et al. (1992)	no	no	no	Zr
gittinsite	$CaZrSi_2O_7$	3.5-4	3.6	Birkett et al. (1992)	yes	yes	yes	Zr
Ti minerals								
aeschynite	$(Y,Ca,Fe)(Ti,Nb)_2(O,OH)_6$	5–6	4.9–9.1	no	yes	no	no	Y
ilmenite	$FeTiO_3$	5–5.5	4.7	Birkett et al. (1996)	no	yes	no	
narsarsukite	$Na_2(Ti,Fe)Si_4(O,F)_{11}$	7	2.7	Miller (1996)	no	no	no	
bafertisite	$Ba(Fe,Mn)_2TiSi_2O_7(O,OH)_2$	5	3.96–4.25	Birkett et al. (1996)	no	no	no	
neptunite	$KNa_2Li(Fe,Mn)_2Ti_2Si_8O_{24}$	5–6	3.23	Birkett et al. (1996)	no	no	no	
aenigmatite	$(Na,Ca)_4(Fe,Ti,Mg)_{12}Si_{12}O_{40}$	5–6	3.7–3.9	Birkett et al. (1996)	no	yes	yes	
astrophyllite	$K_2Na(Fe,Mn)_7Ti_2Si_8O_{26}(OH)_4$	3-3.5	3.3–3.4	Birkett et al. (1996)	yes	no	no	
titanite	$CaTiSiO_5$	5–5.5	3.4–3.56	Miller (1996)	yes	yes	yes	
komarovite	$(Ca,Mn)_2(Nb,Ti)_2Si_2O_7(O,F)_2•3.5(H_2O)$	4	3.61–3.76	no	no	no	yes	Nb
chevkinite	$(Ce,La,Ca,Th)_4(Fe,Mg)_2(Ti,Fe)_3Si_4O_{22}$	5–5.5	4.5	no	no	no	yes	Ce, La, Th
Phosphate minerals								
xenotime	YPO_4	4–5	4.4–5.1	no	no	no	yes	Y
monazite	$(La,Ce,Y,Th)PO_4$	5–5.5	4.8–5.5	Miller (1996)	yes	yes	yes	Ce, La, Y, Th
fluorapatite	$Ca_5(PO_4)_3F$	5.0	3.1–3.2	no	no	yes	no	
apatite	$Ca_5(PO_4)_3(OH,F,Cl)$	5.0	3.2	Gowans et al. (2014)	yes	yes	yes	
britholite	$(Ce,Ca,Th,La,Nd)_5(SiO_4,PO_4)_3(OH,F)$		4.2–4.7	no	yes	no	no	Ce, La, Th
rhabdophane	$(Ce,La)PO_4•(H_2O)$	3.5	4.0	no	no	yes	yes	Ce, La
Other minerals								
gadolinite group	$Be_2(Ca,REE,Fe)_3Si_2O_{10}$	6.5–7	4.2	Miller (1996)	no	no	no	Be, Ce, La, Y
arfvedsonite	$Na_3Fe_4Fe(Si_8O_{22})(OH)_2$	5.5–6	3.44–3.45	Miller (1996)	yes	yes	yes	
aegerine	$NaFe(Si_2O_6)$	6.0	3.5–3.6	Miller (1996)	yes	yes	yes	
pyrochlore	$(Na,Ca)_2Nb_2O_6(OH,F)$	5–5.5	4.2–6.4	Miller (1996)	yes	yes	yes	Nb
bastnaesite	$Ce(CO_3)F$	4-5	4.95–5	Miller (1996)	no	no	yes	Ce
parisite	$Ca(Ce,La)_2(CO_3)_3F_2$	4.5	4.4	no	no	yes	yes	Ce, La
kainosite	$Ca_2(Y,Ce)_2Si_4O_{12}(CO_3)•H_2O$leif	5–6	3.4–3.6	Miller (1996)	no	no	yes	Ce, Y
anthophyllite	$Mg_7(Si_8O_{22})(OH)_2$	5–6	2.9–3.6	no	no	no	yes	
allanite	$(Ce,Ca,Y)_2(Al,Fe)_3(SiO_4)_3(OH)$	5.5	3.3–4.2	Birkett et al. (1992)	yes	no	yes	Ce, Y
milarite	$K_2Ca_4Al_2Be_4Si_{24}O_{60}•(H_2O)$	6	2.52	Gowans et al. (2014)	no	no	no	Be
gerenite	$(Ca,Na)_2(Y,REE)_3Si_6O_{18}•2(H_2O)$	5	3.3–3.52	Jambor et al. (1998)	no	no	no	Ce, La, Nd, Y
leifite	$Na_2(Si,Al,Be)_7(O,OH,F)_{14}$	6	2.57	Sinclair et al. (1992)	no	no	no	Be
danburite	$CaB_2Si_2O_8$	7.0	3.0	no	no	yes	no	
zajacite-(Ce)	$Na(REE_xCa_{1-x})(REE_yCa_{1-y})F_6$ where $(x \neq y)$	3.5	4.4–4.6	Jambor et al. (1996)	no	no	no	Ce, La, Nd
gagarinite-(Y)	$NaCaY(F,Cl)_6$	4.5	4.2	Jambor et al. (1996)	yes	no	no	Y
sphalerlite	$(Zn,Fe)S$	3.5–4	3.9–4.2	Miller (1996)	no	no	no	
molybdenite	MoS_2	1.0	5.5	no	no	yes	no	
galena	PbS	2.5	7.2–7.6	Miller (1996)	no	no	no	
fluorite	CaF_2	4.0	3.0–3.3	Miller (1996)	yes	yes	yes	

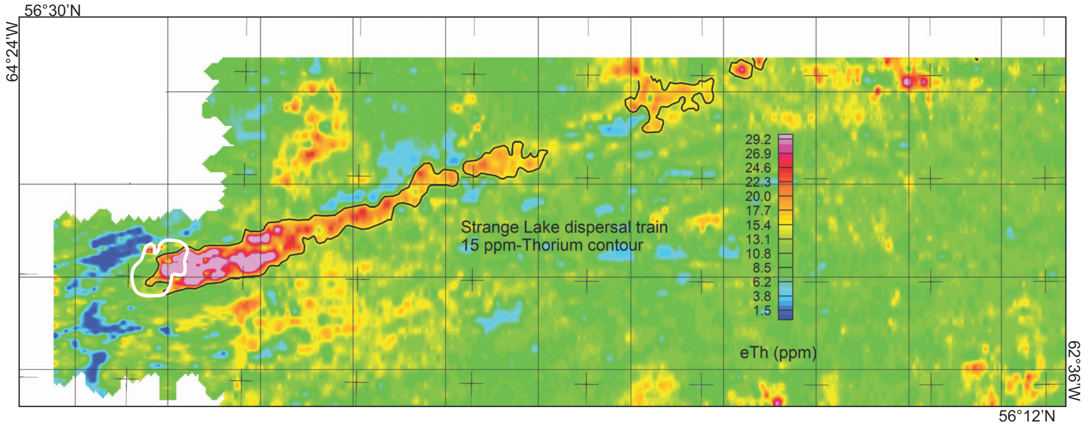

Figure 3. Equivalent Th (ppm) from airborne gamma-ray spectrometry data for the Strange Lake area outlining the northeast-trending zone of high values that reflects the Strange Lake glacial dispersal train. The Strange Lake intrusion is outlined with a white line. Data from Geological Survey of Canada (1980).

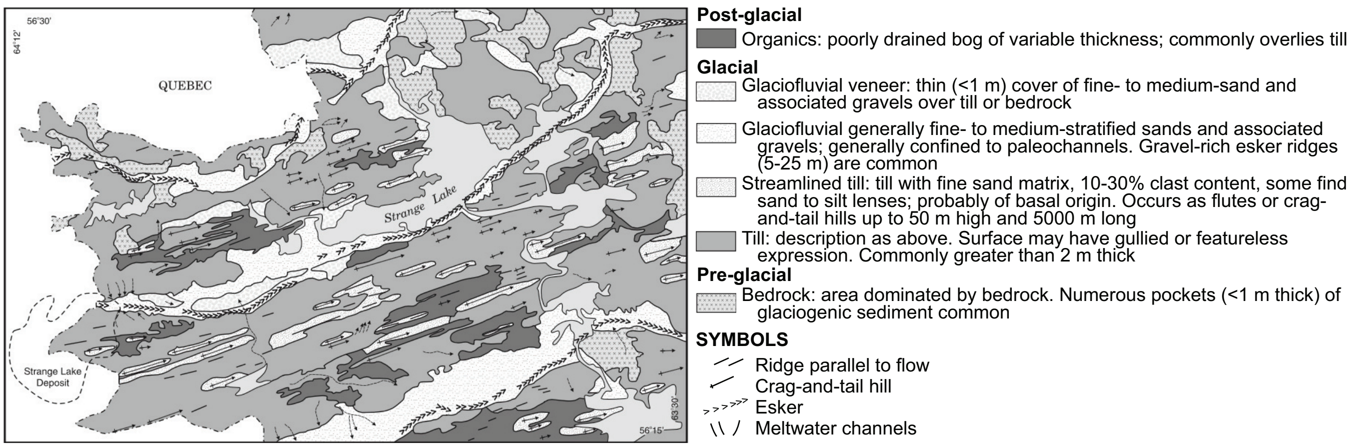

Figure 4. Surficial geology map of the Labrador portion of the Strange Lake area showing a till cover and landforms produced by ice streaming towards the northeast (modified from Batterson (1989) and Batterson and Taylor (2009)).

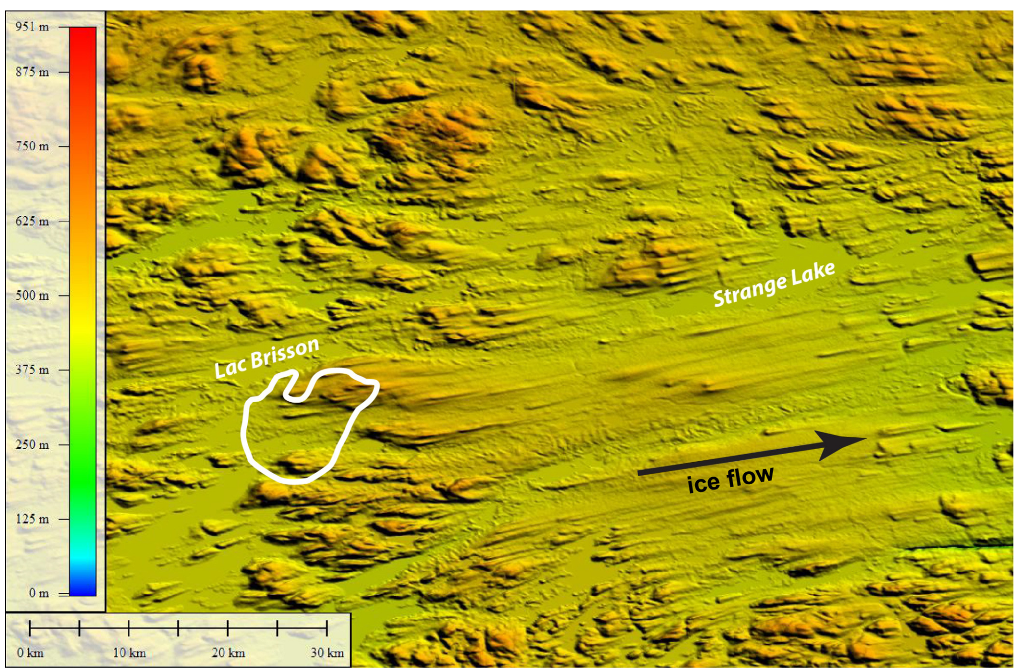

Figure 5. Digital elevation model (DEM) showing the mega-scale glacial lineations from the Kogaluk River ice stream that flowed from left to right (black arrow) across the Strange Lake area. The Strange Lake deposit is shown with a white outline. Image is from the Shuttle Radar Topographic Mission (SRTM).

Figure 6. Photograph of the sandy till that was sampled at site 15-MPB-009 located 50 km down-ice of the Strange Lake intrusion. Note the shovel for scale.

Figure 7. An example of weathered rapakivi granite boulders that are found on the surface overlying and up-ice of the Strange Lake intrusion. This boulder is from till sample site 15-MPB-005 overlying the Strange Lake intrusion. Note the shovel for scale.

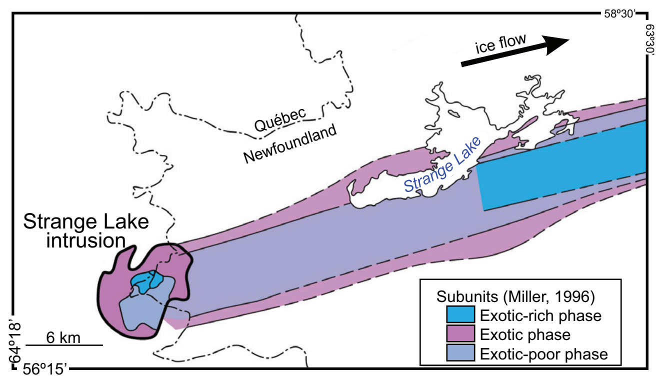

Figure 8. Generalized distribution of mineralized clasts detected at the surface down-ice (east-northeast) of the Strange Lake intrusion. Bedrock subunits in the intrusion and in clasts in till down-ice of the intrusion are shown as three different colours (modified from Batterson, 1989).

glaciofluvial sediments (Fig. 4), including eskers that parallel the dispersal train (Batterson, 1989).

Local till is very sandy (Fig. 6), having been derived mainly from rapakivi granite, located due west of the deposit, as well as from the deposit itself. The till contains, on average, 58% sand, 37% silt, and 5% clay. Numerous highly weathered and disintegrating rapakivi granite boulders from west of the Strange Lake intrusion sit on the till surface up-ice, overlying, and down-ice of the deposit (Fig. 7).

The Laurentide Ice Sheet eroded the Strange Lake intrusion and distributed boulders, cobbles, and glacial sediments in a ribbon-shaped glacial dispersal train (Fig. 8) that can be traced for more than 50 km down-ice to the east-northeast. Elevated concentrations of Be (Fig. 9) Ce, Zr (Fig. 10), La, Nb, Pb, Rb, Th, U, and Y were detected in the ribbon-shaped dispersal train (Batterson, 1989; Batterson and Taylor, 2009).

Previous geochemical studies

In the mid-1980s, the GSC and the Geological Survey of Newfoundland and Labrador completed surficial geochemical studies around the intrusion to document the nature and type of surficial materials, determine the ice-flow history and patterns of glacial dispersal, and determine the surficial geochemical signatures of the intrusion and deposits (Batterson et al., 1985; McConnell and Batterson, 1987; Batterson, 1989; Bolduc, 1990; Batterson and Taylor, 2009). McConnell and Batterson (1987) conducted a multi-media geochemical study around the deposit and reported that indicator elements combined to form a 40 km-long dispersal/dispersion train down-ice (east-northeast) of the deposit with elevated levels of Be, Pb, Nb, La, and Y in till and stream sediments; elevated Y and F in stream water; elevated Be and Pb in lake sediment; and elevated F in lake water. Of these, they concluded that the geochemical patterns in till most clearly defined the dispersal train and indicated the location of the bedrock source.

Bell (1984) and DiLabio (1988, 1995) examined residence sites of metals in till at Strange Lake. They noted that the abundance of Be, Nb, Th, and Zr is greatest in the coarse (2–4 mm) and finest (0.063–0.037 mm) fractions of metal-rich till immediately down-ice of the deposit and that contents of these metals are lower in the intermediate size fractions. They concluded from these patterns that some of the exotic minerals, such as zircon and pyrochlore, are chemically stable in the till, even after post-glacial weathering, and are the source of high metals in the coarse sand fraction.

METHODS

Bedrock sample collection

In the summer of 2008, six bedrock samples were col-

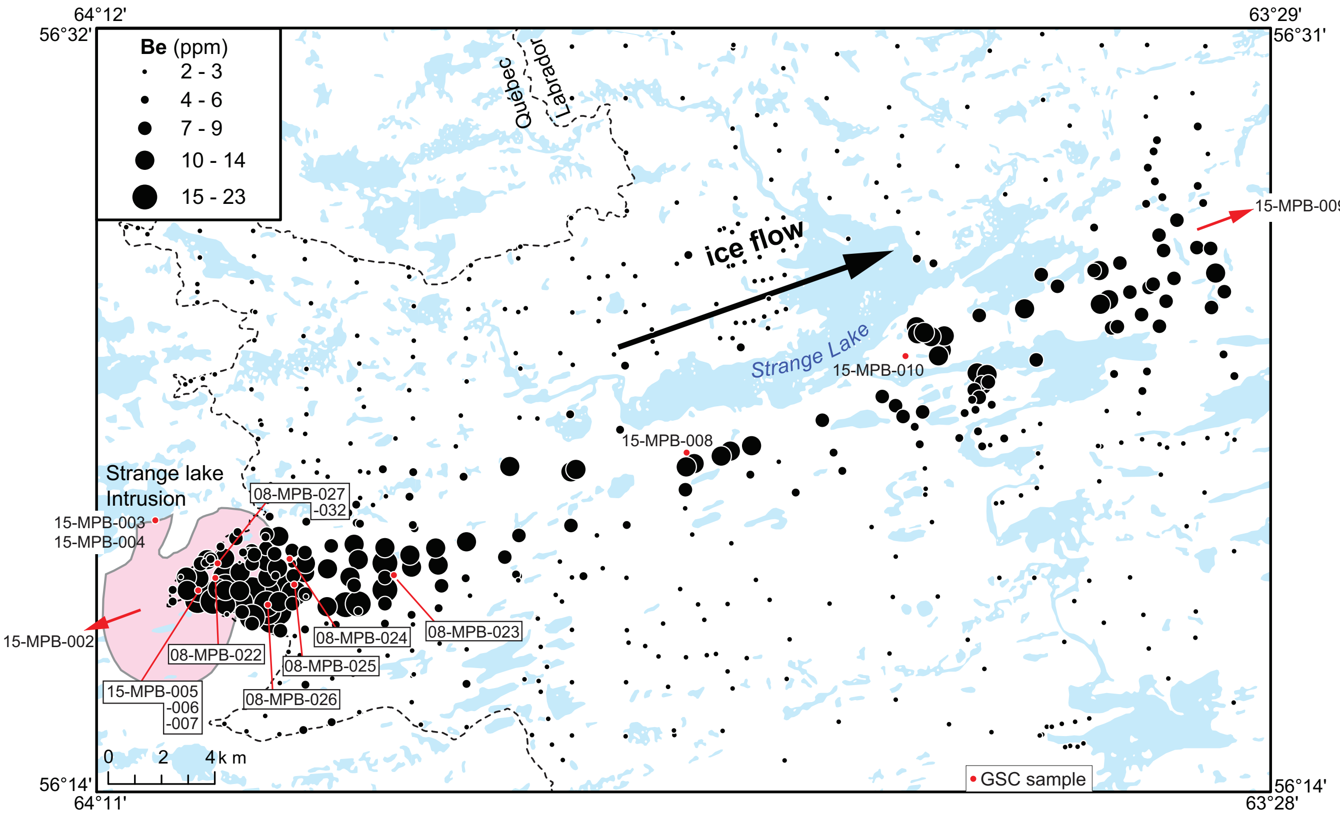

Figure 9. Distribution of Be (ppm) in the <0.063 mm fraction of till (total digestion/ICP-ES) overlying and down-ice of the Strange Lake intrusion (modified from Batterson and Taylor, 2009). Location of GSC bedrock and till samples are shown as red dots. Small red arrows indicate till sample 15-MPB-002, which is located 1 km to the southwest of the map border, and till sample 15-MPB-009, which is located 10 km northeast of the map border.

lected from the Strange Lake Main Zone (samples 08-MPB-027 to -031) by D. Lentz. Colour photographs of polished slabs of each sample are included in Appendix B1, hand sample descriptions are reported in Appendix B2, and petrographic descriptions are included in Appendix B3. In the summer of 2015, four bedrock and one float sample(s) were collected in the Strange Lake area by the GSC. Bedrock sample 15-MPB-003 was collected from a natural bedrock outcrop located on a north-facing slope on the south side of Lac Brisson, which is not part of the B Zone. Bedrock samples 15-MPB-004A-2 and 15-MPB-004B were collected from a stripped outcrop at the B Zone, 86 m to the northwest of sample 15-MPB-003 (Fig. 9). Sample 15-MPB-006 was collected from a natural bedrock outcrop at a high point of land in the central part of the intrusion (Fig. 9). Sample 15-MPB-010A+B is a float cobble suspected to be derived from the Strange Lake complex and glacially transported 30 km down-ice (east) of the deposit (Fig. 9). Colour photographs of the 2015 field sample sites are included in Appendix A2 and colour photographs of the polished slabs of each bedrock sample are included in Appendix B4. Hand sample descriptions of the 2015 samples are reported in Appendix B5 and petrographic descriptions are included in Appendix B6.

Till sample collection

In 1981 and 1983, small (1 kg) till samples were collected by the GSC around the Strange Lake deposit for geochemical analysis of the till matrix (GSC unpubl. data). Till samples were collected from fresh mudboils developed in till at depths of between 0.1 and 0.7 m. Unprocessed dried splits (300 g) of each of these samples were archived at the time of collection. In 2008, a selection of the archived till splits were composited to make five new till samples (08-MPB-022 to -026) for processing to recover indicator minerals. Between five and nine till samples collected in close proximity (within 100 m) were composited into one larger (4 to 7 kg) till sample for recovery of heavy minerals. The original GSC sample numbers and locations for the samples collected in 1981 and 1983, along with resulting composited GSC sample numbers, are listed in Appendix A1. Sample locations are shown in Figure 9.

In the summer of 2015, six large (15 kg) till samples (15-MPB-002, -005, -007 to -010) (Fig. 9) were collected in the Strange Lake area using the dispersal train identified by Batterson and Taylor (2009) as a guide to metal-rich till. Following protocols established by McClenaghan et al. (2013), till samples were collected at depths of between 0.3 to 0.7 m from fresh mudboils

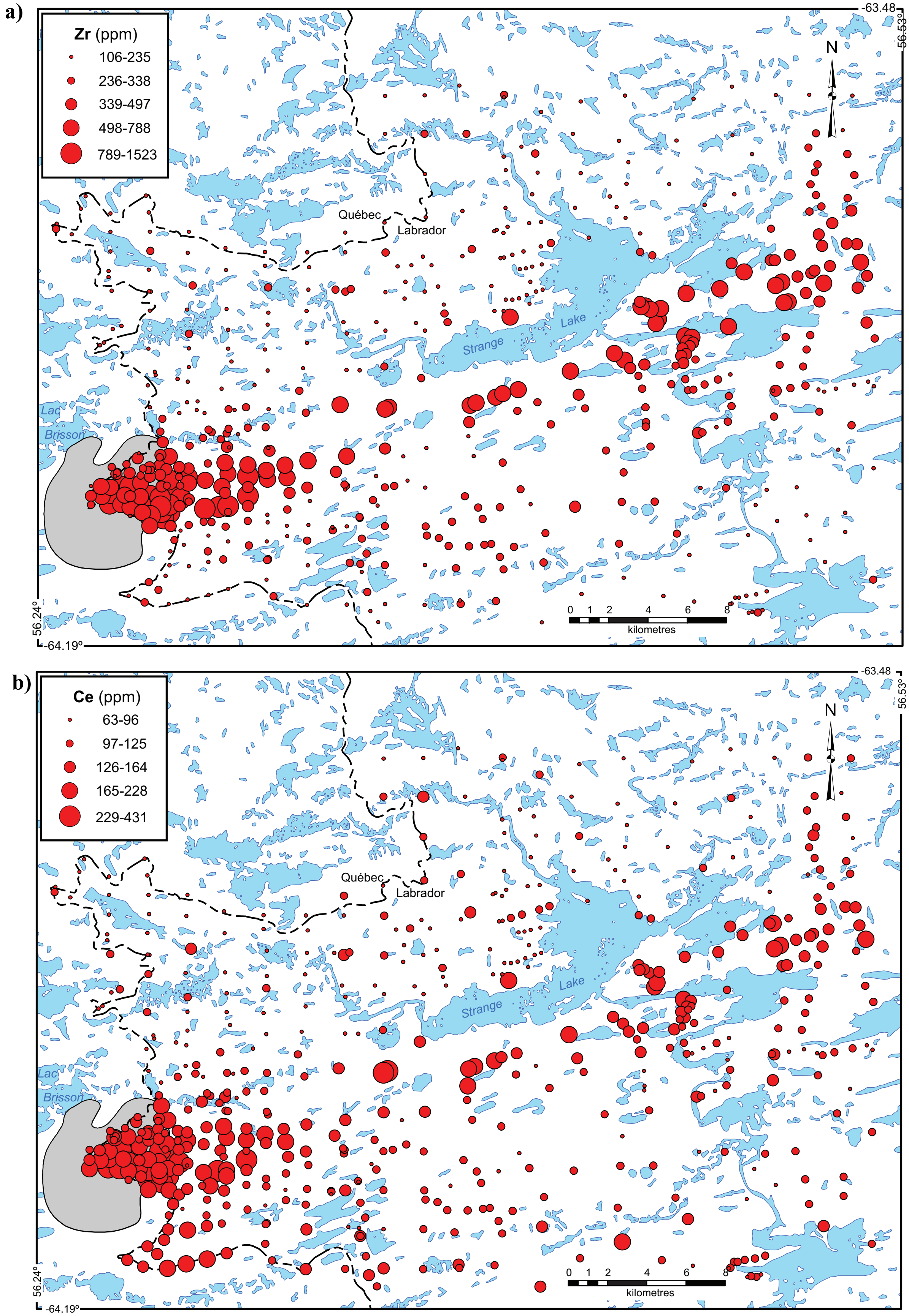

Figure 10. Distribution of **(a)** Zr (ppm) and **(b)** Ce (ppm) in the <0.063 mm fraction of till (4-acid digestion/ICP-ES) overlying and down-ice of the Strange Lake intrusion (grey polygon) (modified from Batterson and Taylor, 2009).

developed in till. Site and sample information are listed in Appendix A1 and site photos are included in Appendix A2. Sample 15-MPB-002 was collected up-ice of the deposit to determine background contents of indicator minerals. Samples 15-MPB-005 and -007 were collected overlying the deposit and samples 15-MPB-008 to -010 were collected between 11 and 50 km down-ice (east-northeast) (Fig. 9).

Sample processing and indicator mineral picking

Four batches of samples were processed at the commercial laboratory Overburden Drilling Management Limited (ODM), Ottawa, to produce heavy mineral concentrates for indicator mineral picking. Batch #1 was submitted to ODM in 2008 and included bedrock samples 08-MPB-027 to -031. ODM lab results for these samples are presented in Appendix C1. Batch #2 was also submitted to ODM in 2008 and included till samples 08-MPB-022 to -026; the results are presented in Appendix C2. Batch #3 was submitted to ODM in 2015 and included bedrock samples 15-MPB-003, -004A-2, -004B, and -006, and float sample 15-MPB-010A; results for these are presented in Appendix C3. Batch #4, also submitted to ODM in 2015, included till samples 15-MPB-002, -005, and -007 to -010; the lab results are presented in Appendix C4. Flow sheets for both bedrock and till sample processing are shown in figures 11 and 12.

Each bedrock sample was visually examined under a binocular microscope and described by geologists at ODM; the samples were then disaggregated using a custom-built CNT Spark-2 electric pulse disaggregator (EPD), rather than a conventional rock crusher, in order to preserve natural grain sizes, textures, and shapes. The material was disaggregated until most fragments were <2 mm in diameter. The weight of material disaggregated ranged from 100 to 400 g (Appendix C.1, C.3).

The <2.0 mm material from each bedrock and till sample was processed using tabling and heavy liquid methods, as described by McClenaghan (2011) and below, to produce a non-ferromagnetic heavy (>3.2 SG) and a mid-density (3.0–3.2 SG) mineral concentrate for examination of indicator minerals. First the <2.0 mm material was passed over a shaking table. The table concentrate was then further refined using heavy liquid separation in methylene iodide diluted to a specific gravity (SG) of 3.2 to produce four fractions: SG >3.2, 3.0–3.2, 2.8–3.0, and <2.8. The SG >3.2 heavy mineral fraction was further refined using a hand magnet to remove the ferromagnetic fraction. The SG >3.2 non-ferromagnetic fraction was sieved into four size fractions: <0.25 mm, 0.25–0.5 mm, 0.5–1.0 mm, and 1.0–2.0 mm. The 0.25–0.5 mm, >3.2 SG fraction was further subjected to paramagnetic separations using a Carpco® magnetic separator at 0.6, 0.8, and 1.0 amps to facilitate mineral identification based on, in part, their magnetic properties.

The SG <3.2 light- to mid-density fraction was further processed using heavy liquid methylene iodide diluted to SG 3.0 to produce two mid-density fractions (SG 2.8–3.0 and 3.0–3.2), however, only the 0.25–0.5 mm fraction of the SG 3.0–3.2 fraction was examined and indicator minerals counted.

The 0.25–0.5, 0.5–1.0, and 1.0–2.0 mm non-ferromagnetic heavy mineral (SG >3.2) and the 0.25–2.0 mm mid-density (SG 3.0–3.2) fractions of bedrock and till samples were then examined with a binocular microscope by trained personnel at ODM and potential indicator minerals of the REE mineralization at Strange Lake, as well as other indicator mineral suites, were counted. Some minerals were removed from the samples and set aside for further analysis.

The visual identification of a limited number of mineral grains was verified with a scanning electron microscope (SEM). Mineral grain abundances in the non-ferromagnetic heavy mineral fraction (SG >3.2) of bedrock and till samples (reported in Appendix C) are listed as raw counts and normalized to a 1 kg sample weight in Table 2. Select mineral abundances in the mid-density (SG 3.0–3.2) fraction of bedrock and till samples are listed in as raw counts and normalized to a 10 kg sample weight in Table 3.

At ODM, quartz ‘blank’ bedrock samples were inserted into bedrock batches #1 (samples 12-MPB-BLK, 12-MPB-1021BLK, 12-CBD-004BLK) and #2 (samples BLANK-1, BLANK-2) to monitor potential cross contamination among samples. The results for the quartz blank samples are reported along with the bedrock samples in McClenaghan et al. (2014) and in Appendix C1 and C2.

Electron microprobe methods

Quantitative mineral analyses were carried out with an automated four-spectrometer Cameca Camebax MBX electron microprobe by wavelength dispersive X-ray analysis method (WDX) at the Earth Sciences Department, Carleton University, Ottawa. Raw X-ray data were converted to elemental weight % by the Cameca PAP matrix correction program. Peak and background positions were carefully selected to avoid instances of peak overlap. A suite of well characterized natural and synthetic minerals and compounds were used as calibration standards (Table 4). Calibration was tested by analyzing known compositions (mineral standards) as unknowns (e.g. zircon). The operating conditions were 20 kV accelerating voltage, 22 nA beam current, focused (2 µm diameter) electron beam. Counting

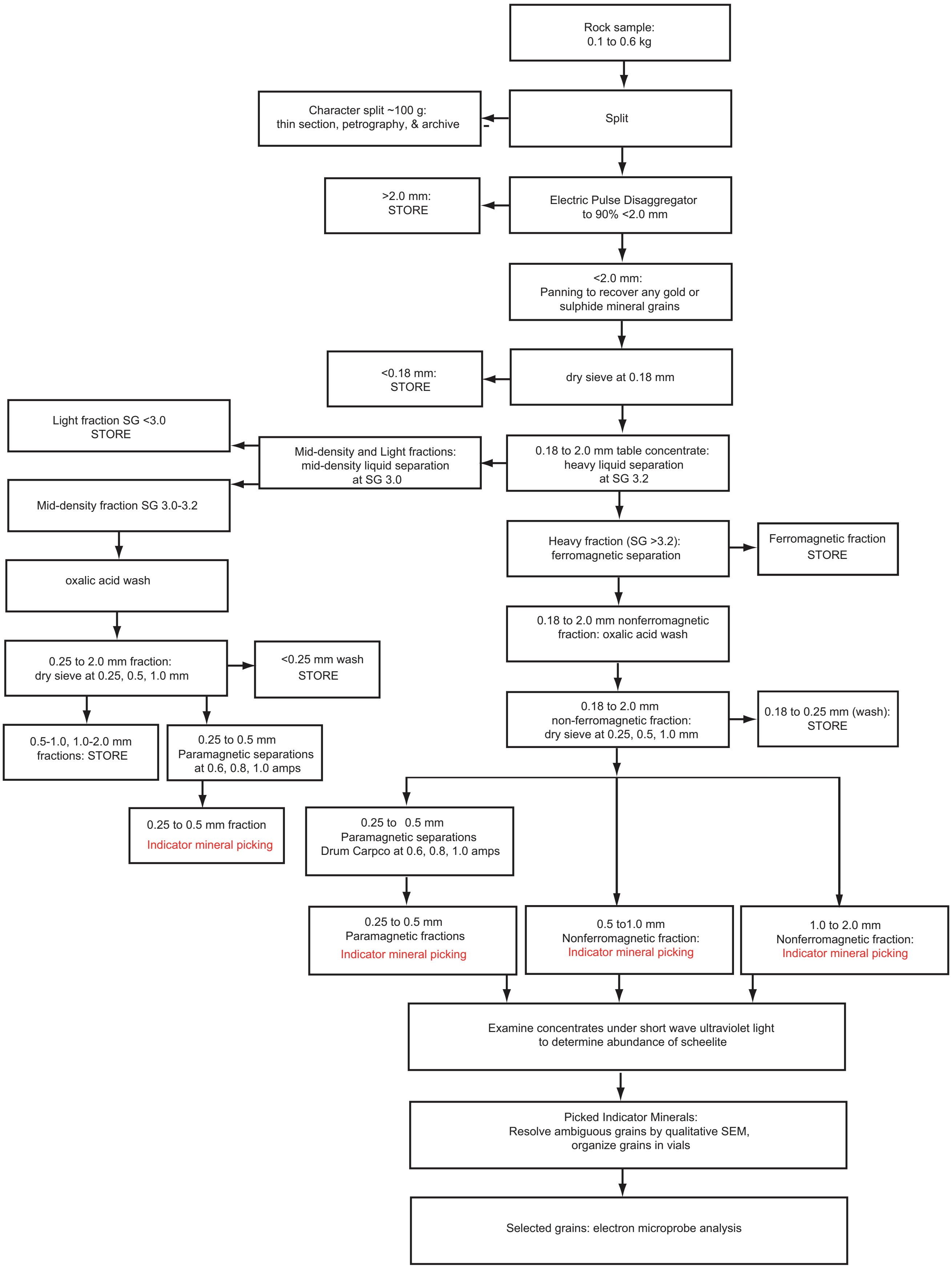

Figure 11. Flow sheet outlining the sample processing and picking procedures used for Strange Lake bedrock samples collected and processed in 2015 at Overburden Drilling Management Limited.

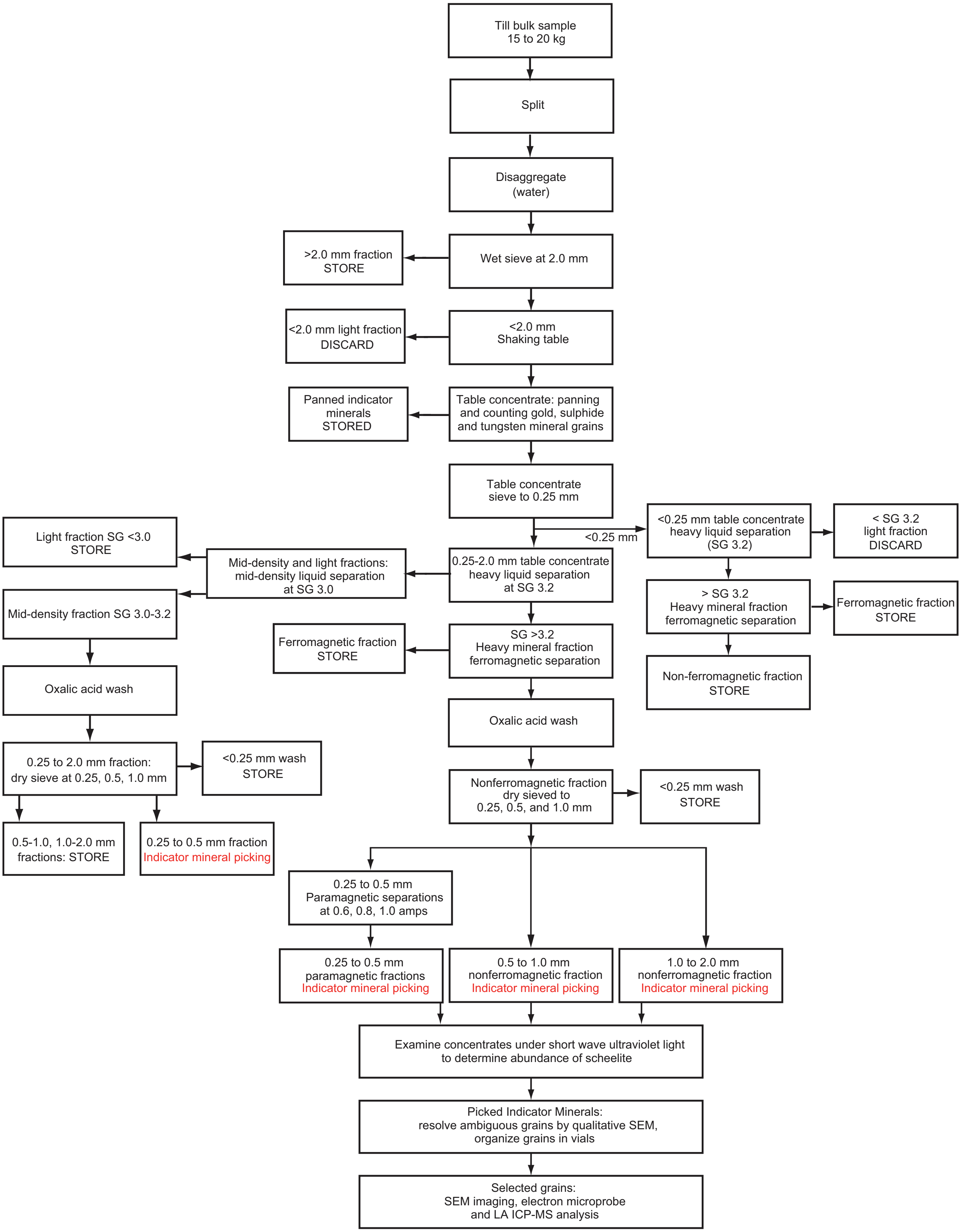

Figure 12. Flow sheet outlining the sample processing and picking procedures used for Strange Lake till samples collected in 1981 and 1983 and processed in 2008, and those collected and processed in 2015.

Table 2. Number of indicator mineral grains in the 0.25 to 0.5 mm non-ferromagnetic heavy mineral fraction (SG >3.2) of bedrock and till samples examined in this study. Mineral grain counts for bedrock are normalized to a 1 kg sample mass of <2 mm (table feed) material. Mineral grain counts for till samples are normalized to a 10 kg mass of the <2 mm (table feed) fraction.

Raw Data

Sample	Location	Material	Mass <2 mm (kg)	Loellingite	Fluorite 3.0-3.2 SG	Titanite	Pyrochlore	Rhabdophane/ monazite	Gittinsite	Parisite	Bastnaesite	Kainosite	Chevkinite	Zircon	Allanite	Thorite/ thorianite	Aegerine	Arfvedsonite
08-MPB-027	Main Zone	bedrock	0.43	13	250	0	36	600	2000	0	0	0	0	1500	0	2	0	15000
08-MPB-028	Main Zone	bedrock	0.25	0	0	2	0	0	0	0	0	0	0	60	0	0	0	3
08-MPB-029	Main Zone	bedrock	0.14	0	250	4000	2	150	3000	0	0	0	0	0	0	1	12000	1000
08-MPB-030	Main Zone	bedrock	0.12	5	80	0	5	12	6	250	0	0	0	0	2	0	2	15000
08-MPB-031	Main Zone	bedrock	0.36	0	0	0	0	0	0	0	0	0	0	3	0	0	0	0
15MPB-006	Main Zone	bedrock	0.79	16	13	0	1	10000	120	0	0	0	0	0	0	2000	30000	8000
15MPB-004B	B Zone	bedrock	0.17	0	250	0	50	0	0	1	0	0	0	10000	10	0	5	0
15MPB-004A02	B Zone	bedrock	0.18	0	1000	0	80	0	0	0	0	0	0	5000	15	0	10000	10
15MPB-003	B Zone	bedrock	0.38	0	50	150	50	3	2	0	0	0	0	0	4000	800	30000	45000
15MPB-010A	35 km down-ice	cobble	0.20	0	0	0	3	200	0	0	0	0	0	80	6	60	2500	25000
08-MPB-022	overlying	till	3.6	0	6	800	2	20	40	1	3	2	0	200	9	4	20	30000
08-MPB-026	1.8 km down-ice	till	4.0	1	0	500	25	100	250	0	7	0	2	1500	2	0	40	50000
08-MPB-025	2.5 km down-ice	till	4.8	3	0	600	12	12	35	0	3	0	23	50	3	0	40	2500
08-MPB-024	3 km down-ice	till	2.2	1	0	800	22	27	100	0	2	10	3	1500	21	3	800	10000
08-MPB-023	5 km down-ice	till	2.7	1	2	250	2	2	120	1	2	0	0	2500	1	0	20	20000
15-MPB-002	2 km up-ice	till	6.3	0	0	300	0	4	0	0	0	0	0	0	0	0	0	0
15-MPB-005	overlying	till	6.2	0	0	15	0	4	5	0	0	0	6	120	1	0	20	60
15-MPB-007	overlying	till	7.2	0	0	15	0	13	3	0	1	0	22	100	1	1	20	200
15-MPB-008	16 km down-ice	till	7.7	4	0	2000	0	4	0	0	0	0	1	700	500	0	20	6000
15-MPB-010	35 km down-ice	till	10.1	0	0	1	5	3	8	0	1	0	6	800	1500	0	50	10000
15-MPB-009	50 km down-ice	till	6.9	2	0	3000	0	4	0	6	1	0	0	150	30	1	100	4000

Normalized data

Sample		Material	Mass <2 mm (kg)	Loellingite	Fluorite 3.0-3.2 SG	Titanite	Pyrochlore	Rhabdophane/ monazite	Gittinsite	Parisite	Bastnaesite	Kainosite	Chevkinite	Zircon	Allanite	Thorite/ thorianite	Aegerine	Arfvedsonite
08-MPB-027	Main Zone	bedrock	0.43	30	582	0	84	1397	4657	0	0	0	0	3492	0	5	0	34924
08-MPB-028	Main Zone	bedrock	0.25	0	0	8	0	0	0	0	0	0	0	237	0	0	0	12
08-MPB-029	Main Zone	bedrock	0.14	0	1822	29155	15	1093	21866	0	0	0	0	0	0	7	87464	7289
08-MPB-030	Main Zone	bedrock	0.12	40	642	0	40	96	48	2005	0	0	0	0	16	0	16	120289
08-MPB-031	Main Zone	bedrock	0.36	0	0	0	0	0	0	0	0	0	0	8	0	0	0	0
15MPB-006	Main Zone	bedrock	0.79	20	16	0	1	12593	151	0	0	0	0	0	0	2519	37779	10074
15MPB-004B	B Zone	bedrock	0.17	0	1463	0	293	0	0	6	0	0	0	58514	59	0	29	0
15MPB-004A02	B Zone	bedrock	0.18	0	5621	0	450	0	0	0	0	0	0	28106	84	0	56211	56
15MPB-003	B Zone	bedrock	0.38	0	132	395	132	8	5	0	0	0	0	0	10535	2107	79010	118515
15MPB-010A	35 km down-ice	cobble	0.20	0	0	0	15	978	0	0	0	0	0	391	29	293	12219	122190
08-MPB-022	overlying	till	3.6	0	17	2222	6	56	111	3	8	6	0	556	25	11	56	83333
08-MPB-026	1.8 km down-ice	till	4.0	3	0	1250	63	250		0	18	0	5	3750	5	0	100	125000
08-MPB-025	2.5 km down-ice	till	4.8	6	0	1250	25	25	73	0	6	0	48	104	6	0	83	5208
08-MPB-024	3 km down-ice	till	2.2	5	0	3636	100	123	455	0	9	45	14	6818	95	14	3636	45455
08-MPB-023	5 km down-ice	till	2.7	4	7	926	7	7	444	4	7	0	0	9259	4	0	74	74074
15-MPB-002	2 km up-ice	till	6.3	0	0	476	0	6	0	0	0	0	0	0	0	0	0	0
15-MPB-005	overlying	till	6.2	0	0	24	0	6	8	0	0	0	10	194	2	0	32	97
15-MPB-007	overlying	till	7.2	0	0	21	0	18	4	0	1	0	31	139	1	1	28	278
15-MPB-008	16 km down-ice	till	7.7	5	0	2597	0	5	0	0	0	0	1	909	649	0	26	7792
15-MPB-010	35 km down-ice	till	10.1	0	0	1	5	3	8	0	1	0	6	792	1485	0	50	9901
15-MPB-009	50 km down-ice	till	6.9	3	0	4348	0	6	0	9	0	0	0	217	43	1	145	5797

bedrock normalized to 1 kg <2 mm; till normalized to 10 kg <2 mm

Table 3. Number of indicator mineral grains in the 0.25 to 0.5 mm non-ferromagnetic mid-density (SG 3.0–3.2) fraction of bedrock and till samples examined in this study.

Sample	Location	Material	Mass <2 mm fraction	Fluorite normalized count	Tourmaline normalized count	Apatite normalized count
08-MPB-027	Main Zone	bedrock	0.43	931	0	0
08-MPB-028	Main Zone	bedrock	0.25	0	0	0
08-MPB-029	Main Zone	bedrock	0.14	7289	0	0
08-MPB-030	Main Zone	bedrock	0.12	1203	0	0
08-MPB-031	Main Zone	bedrock	0.36	0	0	167457
15MPB-006	Main Zone	bedrock	0.79	76	0	0
15MPB-004B	B Zone	bedrock	0.17	3511	0	0
15MPB-004A02	B Zone	bedrock	0.18	8432	0	0
15MPB-003	B Zone	bedrock	0.38	132	0	0
15MPB-010A	35 km down-ice	cobble	0.20	244	0	0
08-MPB-022	overlying	till	3.6	42	56	67
08-MPB-026	1.8 km down-ice	till	4.0	0	50	8
08-MPB-025	2.5 km down-ice	till	4.8	0	42	8
08-MPB-024	3 km down-ice	till	2.2	0	18	18
08-MPB-023	5 km down-ice	till	2.7	19	74	30
15-MPB-002	2 km up-ice	till	6.3	0	32	0
15-MPB-005	overlying	till	6.2	0	21	32
15-MPB-007	overlying	till	7.2	0	17	42
15-MPB-008	16 km down-ice	till	7.7	0	78	130
15-MPB-010	35 km down-ice	till	10.1	0	4	149
15-MPB-009	50 km down-ice	till	6.9	0	3	1159

bedrock normalized to 1 kg <2 mm; till normalized to 10 kg <2 mm

times were 20 seconds or 40,000 accumulated counts. X-ray lines and standards used are listed in Table 4.

RESULTS

Petrography

The petrographic examination of the bedrock samples revealed dark black-green arfvedsonite intergrown with or replaced by aegirine, in a matrix of coarse microcline, albite, and minor olive-green pyrochlore. Various stages of hydrothermal alteration involving aggressive F-rich fluids have dissolved many of the primary minerals and introduced hydrothermal quartz, fluorite, titanite, and rhabdophane, and several secondary Zr-, Y-, Nb-, Ti- and REE-minerals after the dissolution of primary Zr- and Ti-silicates (such as elpidite, which was not observed in these sections). These secondary minerals (including zircon and titanite) have dendritic, plumose, acicular to almost fibrous and globular habits and are intensely intergrown with other hydrothermal minerals such as quartz, fluorite, and hematite and do not form solid euhedral crystals. They occur predominantly in pseudomorphs after primary Zr-minerals (elpidite, armstrongite). (Figs. 13 to 16).

Indicator minerals in bedrock heavy mineral concentrates

Heavy mineral concentrates were made from bedrock samples. The only apparent evidence of indicator mineral carryover during sample preparation is two grains of aegerine from sample 15-MPB-010A (which contains 5% aegerine) that was detected in sample 15-MPB-004B, which is an aegerine-free leucogranite. This carryover likely occurred during tabling or screening of the disaggregated rock and not during disaggregation.

Table 4. Synthetic minerals and compounds, and X-ray lines that were used as calibration standards.

Element	X-ray Line	Material
Si	Ka	natural zircon
Ti	Ka	synthetic $MnTiO_3$
Al	Ka	synthetic $MgAl_2O_4$
Fe	Ka	synthetic Fe_2SiO_4
Mn	Ka	synthetic $MnTiO_3$
Mg	Ka	olivine (Fo92)
Ca	Ka	wollastonite
Na	Ka	albite
K	Ka	microcline
P	Ka	synthetic $ScPO_4$
F	Ka	LiF
Zr	La	natural zircon
Nb	La	synthetic Nb_2O_5
Sn	La	SnO_2
La	La	synthetic $LaAlO_3$
Ce	La	synthetic CeO_2
Pr	Lb	synthetic PrF_3
Nd	Lb	synthetic $NdAlO_3$
Sm	Lb	synthetic $SmAlO_3$
Y	La	synthetic Y-Fe-garnet
Th	Ma	Th-glass

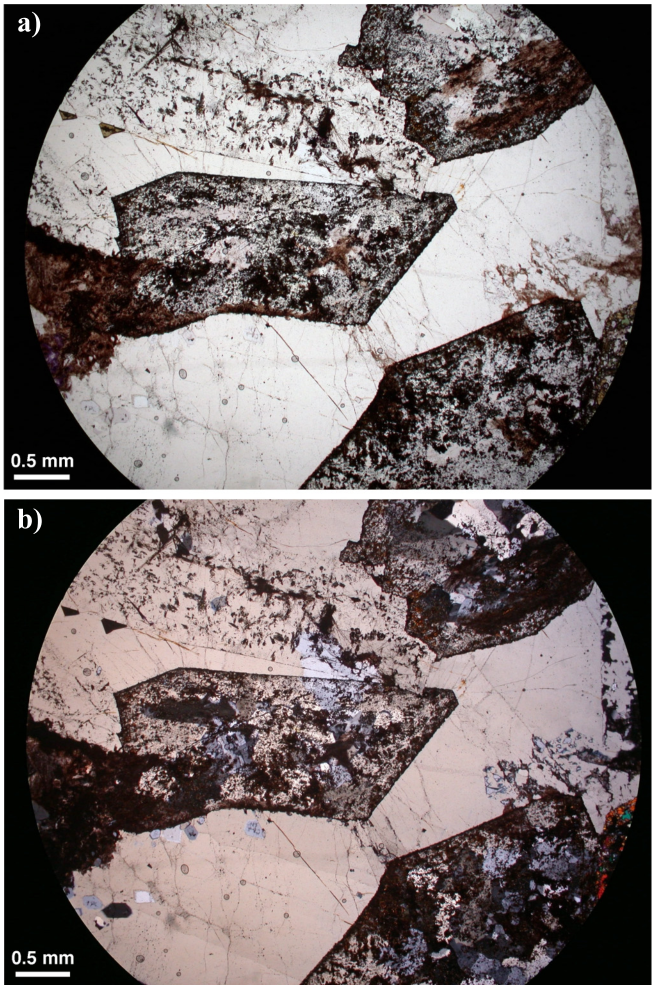

Figure 13. Photomicrographs of bedrock sample 15-MPB-004A-2 showing various pseudomorphs of elpidite(?) containing secondary Zr±Y±Ca-silicates (brown and dark) and hydrothermal quartz (clear). Field of view (F.o.V.) is 4.78 x 6.37 mm and taken using **(a)** plane polarized light and **(b)** crossed polarized light.

Table 1 lists potential indicator minerals of the Strange Lake deposit, which was compiled from published sources and indicator minerals that were observed in bedrock polished thin section (PTS) and heavy mineral concentrate (HMC) in this study. ODM reported that most indicator minerals in bedrock HMC were difficult to visually identify because of their (a) small size; (b) tendency to be intergrown with other indicator minerals and quartz; and (c) discolouration due to hematite staining. The following minerals were particularly difficult to differentiate: 1) thorite and thorianite; 2) rhabdophane and monazite, and 3) zircon and gittinsite. Minerals observed in bedrock samples in this study that were not reported in earlier studies of the Strange Lake deposit include cerianite, uraninite, komarovite, chevkinite, fluorapatite, rhabdophane, parisite, thorianite, danburite, and molybdenite. Colour photographs of some of the minerals recovered from the bedrock samples are shown in Figure 17.

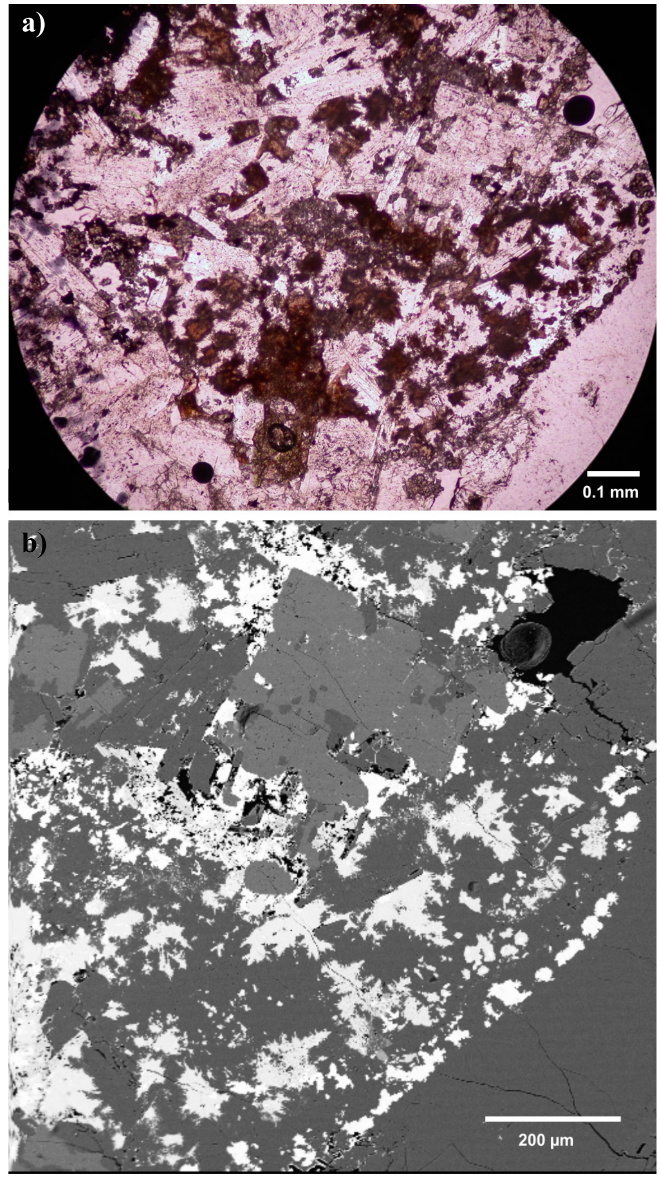

Figure 14. Photomicrographs of bedrock sample 15-MPB-003 showing fuzzy light brown unknown mineral (UM2: Zr-Ca-Y-silicate) and other high-relief secondary Zr-minerals (unknown mineral UM1: Zr-Y-RE-silicate) intergrown with quartz and feldspar in pseudomorph after primary Zr-silicate (elpidite?). Image **(a)** was taken using plane polarized light. The backscatter electron (BSE) image **(b)** shows the Zr-silicates as white, K-feldspar as medium grey, and quartz and albite in darker grey. Field of view (F.o.V.) in both images is 1.10 x 1.47 mm.

Bedrock HMC samples were found to contain few indicator minerals in the 0.25–0.5, 0.5–1.0, or 1.0–2.0 mm fractions other than aegerine, arfvedsonite, fluorite, and zircon because most REE indicator minerals are small (0.1–0.3 mm). Being so small, they are commonly intergrown, resulting in larger grains that are found in the 0.25–2.0 mm picking fractions — most commonly ferriallanite ($CaCe(Fe,Al)_3(SiO_4)(Si_2O_7)O(OH)$), armstrongite ($CaZrSi_6O_{15}\cdot3(H_2O)$), and elpidite ($Na_2ZrSi_6O_{15}\cdot3(H_2O)$. Because the latter two minerals

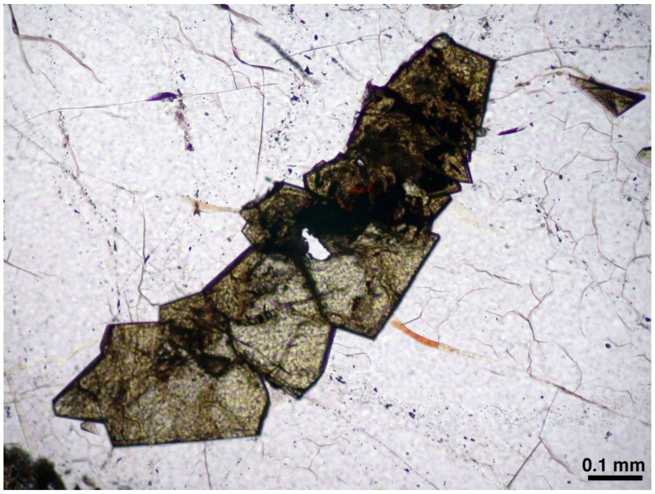

Figure 15. Photomicrograph of bedrock sample 15-MPB-004A02 showing a euhedral pyrochlore aggregate in quartz. Field of view (F.o.V.) is 0.97 x 1.30 mm and was taken using plane polarized light.

have a density of SG 2.7, they were not recovered in the mid-density or heavy fractions that were prepared and examined.

Bedrock sample 15-MPB-R004B contained visible grains of secondary zircon that occurred as powdery white aggregates of minute (1–3 µm) crystals lining vugs left from the dissolution of carbonate minerals.

The only large zircon grains observed were in sample 15-MPB-004A02, which contained 2–5 mm euhedral zircon crystals that comprise 20% of the sample and were found segregated in patches rather than evenly distributed throughout. Only this sample and sample15-MPB-004B yielded large numbers (thousands) of zircon grains when processed, including some grains that are >1 mm.

A few 10s of grains of molybdenite and pyrite were recovered from sample 08-MPB-028. Samples 08-MPB-027 and -030 yielded a few grains of loellingite (NiAs) and sample 08-MPB-031 yielded a few grains of molybdenite. Bedrock sample 15-MPB-006 contained a combined total of 23 grains of molybdenite, sphalerite, and loellingite, and sample 15-MPB-10A contained one grain of molybdenite. In the pan concentrate (<0.25 mm) fraction of the 2015 bedrock samples, the minerals recovered included arsenopyrite, loellingite, and galena.

Bedrock electron microprobe results

Select minerals in the 2008 and 2015 Strange Lake PTS were analyzed by electron microprobe (EMP) to determine some of the more unusual mineral compositions. Data are reported in Appendices D1 and D2. The following minerals were quantitatively analyzed and positively identified: aegirine, arfvedsonite (one Zn- and one Zr-bearing), allanite, zircon, Sn-bearing titanite, monazite, pyrochlore, aeschynite [(Y,Ca,Fe)$(Ti,Nb)_2(O,OH)_6$], gagarinite [$NaCaY(F,Cl)_6$], astrophyllite [$K_2Na(Fe,Mn)_7\ Ti_2Si_8O_{26}(OH)_4$], britholite [$(Ce,Ca,Th,La,Nd)_5\ (SiO_4,PO_4)_3(OH,F)$], and thorite ($ThSiO_4$). In addition, secondary Zr-silicates (unknown minerals UM1, UM2, UM3, and UM8) of varying compositions were observed as replacements of elpidite and gittinsite and showed compositions that did not match any known mineral. Mineral UM1, a Zr-Y-RE-silicate, commonly occurs as fine granular high-relief grains in aggregates in pseudomorphs after elpidite; it is probably a hydrated zircon (see also Zajac, 2015) with additional Y and light RE. UM2 is a CaZr-Y-silicate forming brownish acicular aggregates. Its appearance and composition resemble gittinsite ($CaZrSi_2O_7$), but with Y and some REE substituting for Zr and Ca, respectively, and probably also some additional hydroxyl. The composition of mineral UM3 is very similar to UM1 but it forms small pale yellow globules and is slightly more enriched in Y and RE compared to UM1. Mineral UM5 has the same composition as UM1. Mineral UM8 was found as only one square pale yellow grain intergrown with rhabdophane and is a very SiO_2-rich Zr-silicate with SiO_2 and ZrO_2values similar to armstrongite, but lacking Ca. All these "unknowns" have generally low totals (85–92 wt%), suggesting high OH^- or H_2O content (or the presence of other light elements that were not systematically determined by EMP, such as C, B, Be, or Li) and possibly some additional elements that were not

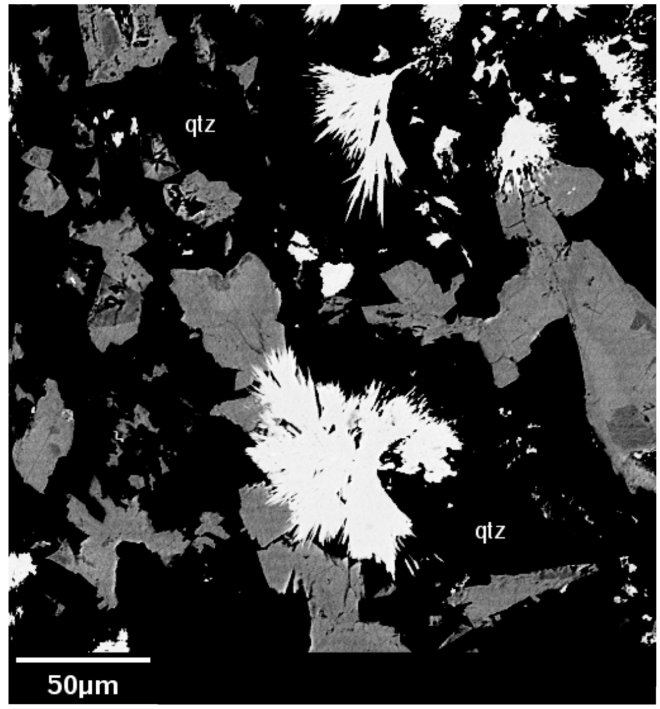

Figure 16. Photomicrograph of bedrock sample 08-MPB-030 showing acicular aggregates of zircon intergrown with gittinsite + quartz in pseudomorphs.

analyzed (e.g. heavy RE, Ba, U, Hf, Zn, Cl); although a check of the EDS spectrum revealed no substantial peaks for any elements other than those that were analyzed.

Eleven pyrochlore grains from the 2008 bedrock samples were analyzed by EMP at Carleton University as part of a B.Sc. thesis by H. Reid (2012). The pyrochlore grains are olive green and euhedral in PTS (Fig. 15), indicating that they formed early in the crystallization sequence of the Strange Lake alkaline granite and did not break down during the subsequent hydrothermal alteration of the granite.

Major to minor element content of the studied pyrochlore grains, in order of abundance, are Nb_2O_5 (51.6–60.7 wt%), Ce_2O_3 (9–11 wt%), Na_2O (2.3–10.7 wt%), CaO (2.01–6.92 wt%), F (0.52–5.35 wt%), TiO_2 (1.28–5.12), La_2O_3 (2.32–4.65 wt%), Ta_2O_5 (0.80–4.16 wt%), Nd_2O_3 (1.58–2.91 wt%), and SiO_2 (0–4.03 wt%) with trace Pb, U, Y, Zr, and others. Strange Lake granitic pyrochlore had distinctively lower Ca/Na ratios than those found in carbonatite (Reid, 2012); Nb and REE levels showed no significant differences.

Indicator minerals in mid-density and heavy mineral concentrates of till samples

Indicator minerals observed in till in this study are listed in Tables 1 to 3. Minerals observed in till samples but not reported in earlier bedrock studies of the Strange Lake deposit include komarovite, chevkinite, parisite, anthophyllite, thorite, thorianite, and rhabdophane. Colour photographs of some of the minerals recovered from the till samples are shown in Figure 17. Select minerals are discussed below. Other less abundant minerals whose presence was noted in the till samples but are not discussed below include kainosite, elpidite, and plumbopyrochlore,

Gittinsite and zircon

Without the use of the SEM to assist with mineral identification, Ca-free zircon ($ZrSi_2O_4$) was difficult to distinguish from Ca-rich gittinsite ($CaZrSi_2O_7$) if the zircon was intergrown with calcite or a REE carbonate mineral such as parisite. Thus, some zircon grains may have been reported as gittinsite.

Tens to hundreds of gittinsite grains are present in till overlying and just down-ice of the deposit (samples 08-MPB-022 to -026) and in till up to 27 km down-ice (samples 15-MPB-008 and -010); the maximum count (625 grains) was found in till sample 08-MPB-0026, collected 1.8 k down-ice (Table 2). None was found in the one till sample collected up-ice. However, till samples were found to contain hundreds to thousands of zircon grains intergrown with gittinsite. Background till sample 15-MPB-002 did not contain zircon.

Rhabdophane/monazite

Rhabdophane $(Ce,La)PO_4{\bullet}(H_2O)$ was difficult to distinguish from monazite $(Ce,La,Nd)PO_4$ thus ODM reported combined counts (Appendix C). Tens to hundreds of the grains are present in till overlying and just down-ice of the deposit as well as in all till samples distally down-ice. A few grains were recovered from the one till sample up-ice. A maximum count of 250 grains was observed in till collected 1.8 down-ice (sample 08-MPB-026, Table 2).

Pyrochlore

Pyrochlore was recognized in HMC by its orange colour and octahedral crystal habit (Fig. 17a). Some grains were checked using the SEM as they resembled staurolite. Tens of grains are present in till overlying and just down-ice of the deposit; none were recovered from the one till sample collected up-ice. The maximum count in till down-ice is 100 grains (sample 08-MPB-024, Table 2).

Bastnaesite

A few grains of bastnaesite were recovered from the HMC of till samples overlying the deposit. Background content is zero grains. The maximum count in till down- ice is 18 grains (sample 08-MPB-026, Table 2). It was identified by its white colour (Fig. 17b) and with assistance from the SEM.

Arfvedsonite

Arfvedsonite was recognized in HMC by its dark reddish brown to black colour and fibrous crystal habit (Fig. 17c). The SEM was used to establish the visual differences between arfvedsonite and hornblende at the start of the examination of all till and bedrock HMC. It is abundant in till; proximal samples contain thousands of grains and more distal samples contain tens to hundreds of grains (Table 2). No arfvdensonite was recovered from background till sample 15-MPB-002.

Aegerine

Aegerine grains were recognized in HMC by their dark green colour and acicular crystals (Fig. 17d). In some cases, the grains were thought to resemble diopside and were checked using the SEM to confirm their identity. Aegerine is present in most till samples. Proximal samples contain tens to thousands of grains and distal samples contain tens of grains. Background sample 15-MPB-002, collected up-ice, does not contain aegerine.

Chevkinite

Chevkinite was visually identified in HMC by its brownish black colour, massive habit, and conchoidal fracture (Fig. 17f). It was identified in five till samples (08-MPB-024, -025, -026, and 15-MPB-08 and -010).

Figure 17. Colour photographs of select indicator minerals from till and bedrock samples collected overlying and down-ice of the Strange Lake deposit: **a)** pyrochlore, till sample 15-MPB-010; **b)** bastnaesite (white) intergrown with allanite (black), till sample 15-MPB-009; **c)** arfvedsonite, till sample 15-MPB-010; **d)** aegerine, till sample 15-MPB-008; **e)** chevkinite, till sample 15-MPB-010; and **f)** fluorite, bedrock sample 15-MPB-004A02. Photographs provided by Michael J. Bainbridge Photography.

One to tens of grains were recovered from both proximal and distal till samples (Table 2). Chevkinite was not recovered from background sample 15-MPB-002 collected up-ice of the deposit.

Allanite

Allanite was visually identified in HMC by its brownish black colour, massive habit, and conchoidal fracture and with assistance from the SEM. In till samples, allanite is intergrown with a whitish mineral. Till samples 15-MPB-008 and -010 contain hundreds of grains (649 and 1485 grains, respectively, Table 2) that consist of allanite intergrown with other minerals. The other till samples contain a few to no grains. Allanite was not recovered from background sample 15-MPB-002.

Parisite

Parasite was visually identified in till HMC by its greyish white colour and with assistance from the SEM. Till samples 08-MPB-022, 15-MPB-023 and -009 contain a few grains of parisite.

Fluorite

Fluorite grains were counted in the 3.0–3.2 SG fraction of till samples. It was easily identified by its deep purple colour (Fig. 17h). It is present in one till sample (08-MPB-022) collected overlying mineralization and is rare to absent in all other till samples (Table 3).

Thorite/thorianite

Thorite and thorianite grains were often intergrown and difficult to differentiate, thus their abundances were reported as a combined total in Table 2 and Appendix C. Proximal samples contain tens of grains and distal samples contain zero to one grain. Background sample 15-MPB-002 collected up-ice does not contain thorite or thorianite.

Titanite

Hundreds of titanite grains are present in background till sample 15-MPB-002 and hundreds to thousands of grains are present in till down-ice (Table 2, Appendix C). Titanite is a common accessory mineral in intermediate and felsic plutonic rocks, and in pegmatite, therefore it is not expected to be any more or less abundant in till down-ice or up-ice of the deposit.

Sulphide and arsenide minerals

Loellingite grains in till HMC were identified by their metallic silver colour and their granular or prismatic habit (Fig. 17e). The identity of several grains was checked using an SEM because of their resemblance to arsenopyrite. Grains were recovered from till samples 08-MPB-023, -024, -025, -026, and 15-MPB-008 and -009 (Table 2). Till sample 08-MPB-024 contained one grain of sphalerite (Appendix C3). Samples 08-MPB-023 and -026 yielded single grains of anglesite (Pb sulphate; Appendix C3).

DISCUSSION

The mineralogy of the Strange Lake granite complex is extremely unusual due to an abundance of primary and secondary Zr-, Y-, RE-, and other high-field strength element (HFSE) minerals. Many of the indicator minerals are very fine grained and strongly altered. For example, bedrock sample 15-MPB-003 contains about 10% REE minerals but the grains are small (<0.3 mm) and consist of heavy minerals, such as allanite, intergrown with lighter minerals, such as armstrongite (SG 2.7) and elpidite (SG 2.54). Thus, these minerals were not documented using routine heavy mineral methods.

Major and minor minerals include quartz, feldspar, arfvedsonite, aegirine, fluorite, Zr-silicates (primary elpidite, secondary gittinsite, and many other hydrated (Zr±Y±Ca) silicates, and pyrochlore. Minerals that appeared both in bedrock (in either PTS and/or bedrock HMC concentrate) and in till collected down-ice from the deposits could be considered as potential indicator minerals, including aegirine, arfvedsonite, apatite, thorite/thorianite, pyrochlore, aenigmatite, fluorite, titanite, monazite/rhabdophane, chevkinite, parisite, gittinsite, and zircon. Elpidite, bastnaesite, and kainosite were not observed in the bedrock samples but were noted in the till HMC; these minerals are likely derived from the Strange Lake deposit and could be potential indicator minerals.

Arfvedsonite and aegirine are common major minerals in sodic alkaline rocks and aenigmatite is a common minor mineral. Although these three minerals are good indicator of the presence of such rocks, they reveal little about the rare metal content. Apatite, titanite, and zircon are common accessory minerals in a wide variety of igneous, metamorphic, and sedimentary rocks and are not specific to this type of rare-metal-rich (NYF-) granite. However, apatite in carbonatite can have distinct trace element signatures that can be diagnostic (e.g. Mao et al., 216); further study of the apatite grains could determine if they are useful indicators of the Strange Lake deposit.

Although zircon and titanite are highly resistate minerals that occur in many common rocks (igneous, metamorphic, sedimentary), their presence is not indicative of a REE-granite. However, in the Strange Lake granite they are secondary minerals and exhibit an unusual acicular to almost fibrous crystal habit that is very different from their usual compact prismatic habit. The fragile aggregates observed here would probably not survive glacial transport and might not actually be derived from the deposit but may possibly be sourced from other country rocks. In the deposit, zircon is often intergrown with gittinsite, making it difficult to differentiate the two. This intergrown form may not only be related to in the Strange Lake deposit but may be indicative of REE mineralization in general. Titanite at Strange Lake is occasionally Sn-bearing but not consistently so; however, this feature may help link titanite grains recovered from till to titanite in the deposit.

Fluorite is another common mineral in F-rich igneous rocks and in hydrothermal assemblages. Its composition is very simple and provides little insight about potential REE mineralization. It is present in the rapakivi granite (Currie, 1985) up-ice as well as in the Strange Lake intrusion, thus its mere presence is of limited value. However, the dark violet colour of the fluorite found in this study is likely due to irradiation from natural sources, suggesting a K-, Th-, or U-rich source; thus, dark fluorite grains may be an indicator mineral for Strange Lake.

Monazite and rhabdophane are both RE-phosphates with very similar compositions (the latter contains H_2O), which makes it difficult to reliably distinguish the two minerals based on EMP or SEM-EDS data alone (O and H cannot be analyzed by these methods). However, their high RE-content makes them useful indicators of the presence of RE-rich rocks. Rhabdophane grains observed in PTS were up to 0.5 mm and subhedral, suggesting it may be a useful indicator mineral for this deposit. It is present in both bedrock and till HMCs.

Parisite has a distinctive reddish brown colour and compact habit and could, if it occurs in sufficiently large grain size, be a useful indicator mineral for RE-rich rocks, such as NYF-granite and certain RE-carbonatite (e.g. Mountain Pass). A few grains were observed in proximal till samples, indicating it may be a useful indicator mineral.

Pyrochlore, which was found in its common primary euhedral phase in the Strange Lake granite, is a valuable ore mineral for Nb. It is very dense and easy to recognize in HMC due to its characteristic octahedral habit. The Strange Lake pyrochlore is olive green in thin section (Fig. 15) but dark to moderate brown to orange in HMC (Fig. 17a). Pyrochlore also occurs in Nb-rich silica-undersaturated alkaline rocks and carbonatite' its presence is always an indicator for high Nb and REE content in the host rocks. Ca/Na ratios can be used to distinguish pyrochlore from Strange Lake-type granitic rocks (low Ca/Na ratio) from those from carbonatite (high Ca/Na) (Reid, 2012). If pyrochlore occurs as sand-size grains, it is a useful indicator mineral (because of its compact habit (usually octahedral), high density, resistate nature, and ease of recognition in HMC.

Thorite and thorianite are heavy dark brown minerals found in pegmatite. In bedrock and till HMC from this study, they were difficult to distinguish and thus were counted and reported as one group. They were observed in HMC of some 2015 bedrock samples (Table 2, Appendix C).

Elpidite is the primary Zr-mineral in the Strange Lake complex and as such it is a key mineral in the deposit. However, in most exposed phases of the complex it has been completely replaced by secondary Zr-silicates and quartz leaving behind boat-shaped pseudomorphs. No fresh elpidite was observed in the bedrock samples examined. Elpidite has a comparatively low density (SG 2.52–2.62), one perfect cleavage, and a splintery fracture, making it a poor indicator mineral and unlikely to survive prolonged transport in glacial environments. Only one grain was observed in one till sample and this one grain was identified only with the aid of an SEM (sample 80-MPB-025, Appendix C3).

Gittinsite is the main replacement mineral of elpidite and is common in the Strange Lake bedrock samples (Table 2). It occurs as very fine-grained acicular to fuzzy aggregates in elpidite pseudomorphs and, in this form, is considered unlikely to survive glacial erosion and prolonged transport. Gittinsite was difficult to visually distinguish from zircon if the zircon was intergrown with calcite or a REE carbonate mineral, such as parisite. Thus, some zircon grains may have been reported as gittinsite. It is present in bedrock and till. It may be a useful indicator mineral proximal (<2 km) to highly altered REE deposits such as Strange Lake.

Chevkinite is a rare REE-silicate that is visually distinct and sufficiently abundant in the till at Strange Lake to be considered a potential indicator mineral. However, it was not identified in the bedrock samples collected in this study. Komarovite was only found in one till sample (08-MPB-024, Appendix C3).

The most useful REE indicator minerals identified in the samples collected within the known Strange Lake dispersal train include gittinsite, zircon, titanite, rhabdophane/monazite, pyrochlore, chevkinite, bastnaesite, kainosite, parisite, and allanite. This list reflects the ability of indicator mineral methods to recover and recognize a broad range of minerals in the >0.25 mm HMC fraction. Colour photographs of some of the minerals are provided here to demonstrate their physical characteristics and facilitate their identification (e.g. colour, cleavage, crystal habit).

Distance of transport

A glacial dispersal train trending east-northeast from the Strange Lake deposit for at least 50 km has been defined using airborne gamma-ray spectrometry,

Table 5. Number of select indicator mineral grains in the 0.25 to 0.5 mm non-ferromagnetic heavy mineral (SG >3.2) fraction of till samples ordered according to the distance down-ice from the Strange Lake Main zone. Mineral grain counts are normalized to a 10 kg sample mass of <2 mm (table feed) material.

Sample	Distance down-ice (km)	Pyrochlore	Fluorite 3.0-3.2 SG	Titanite	Rhabdophane /monazite	Gittinsite	Parisite	Bastnaesite	Kainosite	Chevkinite	Zircon	Allanite	Thorite/ thorianite	Aegerine	Arfvedsonite
15-MPB-002	-2.0	0	0	476	6	0	0	0	0	0	0	0	0	0	0
08-MPB-022	0.0	6	17	2222	56	111	3	8	6	0	556	25	11	56	83333
15-MPB-005	0.0	0	0	24	6	8	0	0	0	10	194	2	0	32	97
15-MPB-007	0.0	0	0	21	18	4	0	1	0	31	139	1	1	28	278
08-MPB-026	1.8	63	0	1250	250	625	0	18	0	5	3750	5	0	100	125000
08-MPB-025	2.5	25	0	1250	25	73	0	6	0	48	104	6	0	83	5208
08-MPB-024	3.0	100	0	3636	123	455	0	9	1136	14	6818	95	14	3636	45455
08-MPB-023	5.0	7	7	926	7	444	4	7	0	0	9259	4	0	74	74074
15-MPB-008	16.0	0	0	2597	5	0	0	0	0	1	909	649	0	26	7792
15-MPB-010	35.0	5	0	1	3	8	0	1	0	6	792	1485	0	50	9901
15-MPB-009	50.0	0	0	4348	6	0	9	0	0	0	217	43	1	145	5797

radioactive boulders, lake sediment geochemistry, and till geochemistry. In fact, one radioactive float cobble (sample 15-MPB-010A) collected 30 km down-ice was confirmed to be from the Strange Lake intrusion by its hydrothermal alteration and indicator mineral content (pyrochlore, rhabdophane, allanite).

Indicator minerals are most abundant in till directly overlying the Strange Lake intrusion and up to 3 to 5 km down-ice (Table 5). However, a few grains of pyrochlore, gittiinste, bastnaesite, and chevkinite were detectable in till up to 35 km down-ice within the known dispersal train, and a few grains of rhabdophane, parisite and allanite were observed in one till sample collected 50 km down-ice (sample 15-MPB-009, Table 2).

Comparison to other till studies

The results reported here greatly expand on the earliest observations of indicator minerals in till at Strange Lake by Bell (1984) and DiLabio (1988, 1995). The results are also consistent with those recently reported by Wilton et al. (2017) for till collected 100 km down-ice (east-northeast) of Strange Lake. These authors identified gittinsite grains in the 0.125 to 0.180 mm heavy mineral fraction, which they interpreted to be have been glacially transported eastward from the Strange Lake deposit. Their study demonstrates that visual examination of the coarse >0.25 mm fraction can indeed identify a broad range REE-bearing minerals.

The suite of REE indicator minerals identified for Strange Lake includes some of those reported for till in eastern and northern Finland by Lehtonen et al. (2011) and Sarappää and Sarala (2013). These authors observed varying combinations of pyrochlore, columbite-tantalite, monazite, xenotime, allanite, and rhabdophane which they interpreted to be derived from REE-rich bedrock.

Advantages of using indicator mineral methods

Using indicator minerals for REE exploration has many advantages: 1) the method described here is well established and has been used by industry and governments for more than 30 years and thus results can be compared among surveys conducted during different years or by different organizations; 2) the method is fast and moderately priced; 3) identification of REE-minerals can be conducted as part of any indicator mineral survey undertaken for other commodities, i.e., precious and base metal exploration.

The advantages of visually examining the >0.25 mm fraction of till to identify indicator minerals rather than using geochemical analysis are that the indicator mineral grains (1) are visible and can be examined with a binocular or scanning electron microscope; (2) are sufficiently large that they may be manipulated without being mounted, which allows their 3-dmiinersional shape and surface textures to be examined; (3) may be chemically analyzed to provide information about the nature of the mineralizing system; (4) provide physical evidence of the presence or absence of mineralization or alteration; (5) may be present in very low abundances (a few grains in a 10 kg till sample) that are readily detectable by indicator mineral methods but not by till geochemical methods (Averill, 2001; McClenaghan, 2011).

Indicator mineral methods have been used in exploration programs and government geochemical surveys to evaluate the potential of a region or large property to host a variety of commodities, including diamonds (McClenaghan and Kjarsgaard, 2007), gold (McClenaghan and Cabri, 2011), Ni-Cu-PGE, porphyry Cu, VMS-hosted Cu-Pb-Zn, and granite-hosted Cu-Mo and Sn-W (Averill, 2001, 2011; McClenaghan et al., 2015b, 2016, 2017; Plouffe et al., 2016). Rare earth element indicator minerals may now be added to this expanding list of commodities that can be targeted in all exploration programs. When focused on property-scale targets, indicator mineral methods should be used in combination with till geochemistry to explore mineralization properties and/or follow up anomalies.

CONCLUSIONS

This study is the first detailed investigation of the indicator mineral signature of a major REE deposit in glaciated terrain. The Strange Lake deposit contains numerous oxide, silicate, phosphate, and carbonate indicator minerals, with some being observed in till up to 50 km down-ice. A number of the indicator minerals were noted in the bedrock samples (cerianite, uraninite, aeschynite, fluorapatite, britholite, danburite, molybdenite), and others in the till samples (komarovite, chevkinite, xenotime, anthophyllite), and some were present in both the bedrock and till samples (thorianite, rhabdophane, parisite). Many of these indicator minerals had not been previously reported for the Strange Lake deposit

The most useful indicator minerals of the Strange Lake intrusion and its REE mineralization include Zr-silicates (secondary gittinsite and many other hydrated Zr±Y±Ca-silicates), pyrochlore, thorite/thorianite, monazite/rhabdophane, chevkinite, parisite, bastnaesite, kainosite, and allanite.

The Strange Lake test site is exceptional for two reasons. First, a large volume of material was glacially eroded from the deposit and second, the debris was glacially transported a long distance by an ice stream. The net result is an extremely long ribbon-shaped dispersal train. The remarkable Strange Lake train was ideal for collecting REE-rich till at varying distances down-ice to test and develop REE indicator mineral methods. The indicator mineral abundances for till reported here offer a guide to what might be expected in till proximal and distal to REE mineralization in this region, and elsewhere.

This case study demonstrates that REE indicator minerals can now be added to a large collection of indicator minerals that may be used to explore for a broad range of deposit types and commodities. This suite of REE minerals can be recovered from the till or stream sediment samples, regardless of whether they were collected for diamond, precious metal, base metal, or strategic metal exploration.

ACKNOWLEDGEMENTS

This study was initiated as part of the Geological Survey of Canada’s (GSC) Targeted Geoscience Initiative (TGI-3) Program and completed as part of the GSC’s Geo-mapping for Energy and Minerals (GEM-2) Program (2014-2018) in the Hudson-Ungava region. The 2008 bedrock samples were collected by D. Lentz in collaboration with A. Williams-Jones. The authors acknowledge Quest Rare Minerals Limited, in particular E. Walker and J. Renaud, for providing access to the Strange Lake property in 2015. H. Dubé-Loubert, Ministère de l'Énergie et des Ressources naturelles du Québec, and J. Rice, Ph.D. candidate at the University of Waterloo, are thanked for providing assistance with the collection of till and bedrock samples in 2015. Discussions with R.N.W. DiLabio and S. Zajac were helpful to this research. I. McMartin (GSC) is thanked for her review of this manuscript. Page layout was completed by E. Ambrose.

REFERENCES

Averill, S.A., 2001. The application of heavy indicator minerals in mineral exploration with emphasis on base metal indicators in glaciated metamorphic and plutonic terrain, *In:* Drift Exploration in Glaciated Terrain, (eds) M.B. McClenaghan, P.T. Bobrowsky, G.E.M. Hall, and S. Cook; Geological Society of London, Special Volume 185, p. 69–82.

Averill, S.A., 2011. Viable indicators in surficial sediments for two major base metal deposit types: Ni-Cu-PGE and porphyry Cu; Geochemistry: Exploration, Environment, Analysis, v. 11, p. 279–291.

Batterson, M.J., 1989. Glacial dispersal from the Strange Lake alkalic complex, northern Labrador, *In:* Drift Prospecting, (eds) R.N.W. DiLabio and W.B. Coker; Geological Survey of Canada, Paper 89-l20, p. 31–40.

Batterson, M.J. and Taylor, D.M., 2005a. Landforms and surficial geology of the NTS 14D/05 map sheet (untitled); Newfoundland and Labrador Department of Mines and Energy, Geological Survey, Map 2003-27, Scale: 1:50 000. Open File 014D/05/0247.

Batterson, M.J. and Taylor, D.M., 2005b. Landforms and surficial geology of the Lac Dihourse map sheet (NTS 24A/08); Government of Newfoundland and Labrador, Department of Mines and Energy, Geological Survey, Map 2003-28, Scale: 1:50 000. Open File 024A/08/0027.

Batterson, M.J. and Taylor, D.M., 2009. Geochemical re-analysis of till samples from the Strange Lake area, Labrador (NTS Map Sheets 14D/5 and 24A/8); Newfoundland and Labrador Department of Natural Resources, Geological Survey, Open File LAB/1479.

Batterson, M.J., Taylor, D.M., and Vatcher, S.V., 1985. Quaternary mapping and drift exploration in the Strange Lake areas, Labrador, In: Current Research; Newfoundland and Labrador Department of Mines and Energy, Mineral Development Division, Report 85-1, p. 4–10.

Bell, J.E., 1984. Mineralogy of till in a dispersal train derived from a peralkaline granite, Lac Bisson, Quebec-Newfoundland; B.Sc. Thesis, Queen's University, 30 p.

Birkett, T.C., Miller, R.R., Roberts, A.C., and Mariano, A.N., 1992. Zirconium-bearing minerals of the Strange Lake intrusive complex, Quebec-Labrador; The Canadian Mineralogist, v. 30, p. 191–205.

Birkett, T.C., Trzcienski, W.E., and Stirling, J.A.R., 1996. Occurrence and compositions of some Ti-bearing minerals in the Strange Lake intrusive complex, Quebec-Labrador boundary. The Canadian Mineralogist, v. 34, p. 779-801.

Bolduc, A., 1990. Dispersion, dans les sédiments glaciaires et fluvio-glaciaires, des débris en provenance du granite hyperalcalin de Strange Lake, Labrador, *In:* Application de la géologie du Quaternaire à l'exploration minérale : cours intensif, (eds) S. Averill, A. Bolduc, W.B. Coker, R.N.W. DiLabio, M. Parent, and J. Veillette; Association professionelle des géologues et des géophysiciens du Québec, Congrès de l'Association professionnelle des géologues et des géophysiciens du Québec; Sainte-Foy, Québec, 29-30 mars 1990, p. 108–138.

Chakhmouradian, A.R. and Wall, F., 2012. Rare earth elements: minerals, mines, magnets (and more); Elements, v. 8, p. 333–340.

Currie, K.L., 1985. The unusual peralkaline granite near Lac Brisson, Quebec-Labrador, *In:* Current Research; Geological Survey of Canada, Report 85-1A, p. 73–90.

DiLabio, R.N.W., 1988. Residence sites of gold, PGE and rare lithophile elements in till, *In:* Prospecting in Areas of Glaciated Terrain – 1988, (eds) D.R. McDonald and K.A. Mills; Canadian Institute of Mining and Metallurgy, p. 121–140.

DiLabio, R.N.W., 1995. Residence sites of trace elements in oxidized till, *In:* Drift Exploration in the Canadian Cordillera, (eds.) P.T. Bobrowsky, S.J. Sibbick, J.M. Newell, and P.F. Matysek; British Columbia Ministry of Energy, Mines and Petroleum Resources, Paper 1995-2, p. 67–76.

Dyke, A.S. and Prest, V.K., 1987. Late Wisconsin and Holocene history of the Laurentide Ice Sheet; Géographie physique et Quaternaire, v. 41, p. 237–263.

Geological Survey of Canada, 1980. Airborne gamma ray spectrometric map, Dihourse Lake Quebec-Newfoundland. Geological Survey of Canada, Geophysical Series, Map 35124(08)G.

Gowans, R.M., Lewis, W.J., Shoemaker, S., Spooner, J., and Zalnieriunas, R.V., 2014. Quest Rare Minerals Ltd. NI-43-101 Technical report on the preliminary economic assessment (PEA) for the Strange Lake Property, Quebec, Canada; Micon International Limited, www.SEDAR.com.

Hatch, G.P., 2012. Rare earth elements: dynamics in the global market for rare earth; Elements, v. 8, p. 341–46.

Hornbrook, E.H.W., Maurice, Y.T., and Lynch, J.J., 1979. Regional lake sediment and water geochemical reconnaissance data, Labrador; Geological Survey of Canada, Open File 559.

Jambor, J.L., Roberts, A.C., Owens, D.R., and Grice, J.D., 1996. Zajacite-(Ce), a new rare-earth fluoride from the Strange Lake deposit, Quebec-Labrador; The Canadian Mineralogist, v. 34, p. 1299–1304.

Jambor, J.L., Roberts, A.C., Grice, J.D., Birkett, T.C., Groat, L., and Zajac, S., 1998. Gerenite-(Y), $(CaNa)_2(Y,REE)_3Si_6O_{18}\cdot 2H_2O$, a new mineral species and an associated Y-bearing gadolinite-group mineral, from the Strange Lake peralkaline complex, Quebec-Labrador; The Canadian Mineralogist, v. 36, p. 793–800.

Kerr, A., 2013. Rare-Earth-Element (REE) behaviour in the Strange Lake intrusion, Labrador: resource estimation using predictive methods, In: Current Research; Newfoundland and Labrador Department of Natural Resources, Geological Survey Report 13-1, p. 117-136.

Kerr, A. and Rafuse, H., 2012. Rare-earth element (REE) behaviour in the Strange Lake intrusion: resource estimation using predictive methods, *In:* Current Research; Newfoundland and Labrador Department of Natural Resources, Geological Survey Report 12-1, p. 39–60.

Lehtonen, M., Laukkanen, J., and Sarala, P., 2011. Exploring RE and REE mineralization using indicator minerals, *In:* Indicator Mineral Methods in Mineral Exploration, Workshop 3, (conv.) B. McClenaghan, V. Peuraniemi, and M. Lehtonen; Association of Applied Geochemists, p. 13–18.

Mackay, D.A.R. and Simandl, G.J., 2015. Pyrochlore and columbite-tantalite as indicator minerals for specialty metal deposits; Geochemistry: Exploration, Environment, Analysis. v. 15, p. 167–178.

Margold, M., Stokes, C.R., Clark, C.D., and Kleman, J., 2015. Ice streams in the Laurentide Ice Sheet: a new mapping inventory; Journal of Maps, v. 11, p. 380–395.

McClenaghan, M.B., 2011. Overview of common processing methods for recovery of indicator minerals from sediment and bedrock in mineral exploration; Geochemistry: Exploration, Environment, Analysis, v. 11, p. 265–278.

McClenaghan, M.B. and Cabri, L.J., 2011. Gold and platinum group element indicator minerals in surficial sediments; Geochemistry: Exploration, Environment, Analysis, v. 11, p. 251–263.

McClenaghan, M.B. and Kjarsgaard, B.A., 2007. Indicator mineral and surficial geochemical exploration methods for kimberlite in glaciated terrain: Examples from Canada, *In:* Mineral Deposits of Canada: A Synthesis of Major Deposit Types, District Metallogeny, the Evolution of Geological Provinces, and Exploration Methods, (ed.) W.D. Goodfellow; Geological Association of Canada, Mineral Deposits Division, Special Publication No. 5, p. 983–1006.

McClenaghan, M.B., Plouffe, A., McMartin, I., Campbell, J.E., Spirito, W.A., Paulen, R.C., Garrett, R.G., and Hall, G.E.M., 2013. Till sampling and geochemical analytical protocols used by the Geological Survey of Canada; Geochemistry: Exploration, Environment, Analysis, v. 13, p. 285–301.

McClenaghan, M.B., Paulen, R.C., Rice, J.M., Sanborn-Barrie, M., McCurdy, M. W., Spirito, W.A., Adcock, S., Veillette, J.J., Garrett, R.G., Grunsky, E.C., Pickett, J., Layton-Matthews, D., and Corrigan, D., 2014. GEM 2 Hudson-Ungava Project: southern Core Zone surficial geology, geochemistry, and bedrock mapping activities in northern Quebec and Labrador; Geological Survey of Canada, Open File 7705.

McClenaghan, M.B., Paulen, R.C., Rice, J.M., McCurdy, M. W., Fortin, R., Spirito, W.A., Adcock, S., Ross, M., Pyne, M., and Dubé-Loubert, H., 2015a. Report of activities for the Core Zone: 2015 surficial geology, geochemistry, and gamma-ray spectrometry studies in northern Quebec and Labrador; Geological Survey of Canada, Open File 7946.

McClenaghan, M.B., Paulen, R.C., Layton-Matthews, D., Hicken, A.K., and Averill, S.A., 2015b. Glacial dispersal of gahnite from the Izok Lake Zn-Cu-Pb-Ag VMS deposit, northern

Canada. Geochemistry: Exploration, Environment, Analysis, v. 15, p. 333–349.

McClenaghan, M.B., Parkhill, M.A., Pronk, A.G., and Sinclair, W.D., 2016. Indicator mineral signatures of Sn-W deposits: examples from the Mount Pleasant Sn-W-Mo-Bi-In deposit, New Brunswick, Canada; Journal of Geochemical Exploration, v. 172, p. 151–166.

McClenaghan, M.B., Parkhill, M.A., Pronk, A.G., Seaman, A.A., McCurdy, M., and Leybourne, M.I., 2017. Indicator mineral and geochemical signatures associated with the Sisson W-Mo deposit, New Brunswick, Canada; Geochemistry: Exploration, Environment, Analysis. published online first 10.1144/geochem2015-396.

McConnell, J.W. and Batterson, M.J., 1987. The Strange Lake Zr-Y-Nb-Be-REE deposit, Labrador: a geochemical profile in till, lake and stream sediment, and water; Journal of Geochemical Exploration, v. 29, p. 105–127.

Miller, R.R., 1986. Geology of the TRange Lake alkali complex and the associated Zr-Y-Nb-Be-REE mineralization, *In:* Current Research 1986; Newfoundland and Labrador Department of Mines and Energy, Report 86-1, p. 11–19.

Miller, R.R., 1988. Yttrium (Y) and other rare metals (Be, Nb, REE, Ta, Zr) in Labrador, In: Current Research 1988; Newfoundland and Labrador Department of Mines and Energy, Report 88-1, p. 229–245.

Miller, R., 1990. The Strange Lake pegmatite-aplite-hosted rare-metal deposit, Labrador. Current Research 1990; Newfoundland and Labrador Department of Mines and Energy, Report 90-1, p. 171–182.

Miller, R.R., 1996. Structural and textural evolution of the Strange Lake peralkaline rare-element (NYF) granite pegmatite, Quebec-Labrador; The Canadian Mineralogist, v. 34, p. 349–371.

Miller, R.R., Heaman, L.M., and Birkett, T.C., 1997. U-Pb zircon age of the Strange Lake peralkaline complex: implications for Mesoproterozoic peralkaline magmatism in north central Labrador; Precambrian Research, v. 81, p. 67–82.

Paulen, R.C., Stokes, C.R., Fortin, R., Rice, J.M., Dubé-Loubert, H., and McClenaghan, M.B. 2017. Dispersal trains produced by ice streams: an example from Strange Lake, Labrador, Canada, *In:* Proceedings of the Sixth Decennial International Conference on Mineral Exploration.

Plouffe, A., Ferbey, T., Hashmi. S., and Ward. B.C., 2016. Till geochemistry and mineralogy: vectoring towards Cu porphyry deposits in British Columbia, Canada; Geochemistry: Exploration, Environment, Analysis, v. 16, p. 213–232.

Reid, H., 2012. Pyrochlore as an indicator mineral for rare earth elements; B.Sc. thesis, Carleton University, Ottawa, Ontario, 30 p.

Roelofson, J.N. and Veblen, D.R., 1999. Relationships among zirconosilicates: examination by cathodoluminescence and transmission electron microscopy; Mineralogy and Petrology, v. 67, p. 71–84.

Sarappää, O. and Sarala, P., 2013. Rare earth element and gold exploration in glaciated terrain: example from the Mäkärä area, northern Finland; Geochemistry: Exploration, Environment, Analysis, v. 13, p. 131–143.

Simandl, G.J., 2014. Geology and market-dependent significance of rare earth element resources; Mineralium Deposita, v. 49, p. 889–904.

Simandl, G.J., Prussin, E.A., and Brown, N., 2012. Specialty metals in Canada; British Columbia Geological Survey, Open File 2012-7.

Simandl, G.J., Mackay, D.A.R., Ma, X., Luck, P., Gravel, J. Grcic, B., and Redfearn, M., 2015. Direct and indirect indicator minerals in exploration for carbonatites and related ore deposits — an orientation survey, British Columbia, Canada, *In:* Application of Indicator Mineral Methods to Exploration; Association of Applied Geochemists, Short Course 2, p. 32–39.

Sinclair, W.D., Jambor, J.L., and Birkett, T.C., 1992. Rare earths and the potential for element deposits in Canada; Exploration and Mining Geology, v. 1, p. 265–281.

Verplanck, P.L. and Van Gosen, B.S., 2011. Carbonatite and alkaline intrusion-related rare earth element deposits — a deposit model; Unite States Geological Survey, Open-File Report 2011-1256.

Vincent, J.S., 1989. Quaternary geology of the southeastern Canadian Shield, *In:* Chapter 3 of Quaternary Geology of Canada and Greenland, (ed.) R.J. Fulton; Geological Survey of Canada, Geology of Canada, no. 1 (also: Geological Society of America, The Geology of North America, v. K-1).

Wilton, H.C., Thompson, G.M., and Grant, D.C., 2017. The use of automated indicator mineral analysis in the search for mineralization – A next generation drift prospecting tool; EXPLORE, Association of Applied Geochemists, no. 174, p. 1–18.

Zajac, S.I., 2015. John Jambor's contributions to the mineralogy of the Strange Lake peralkaline complex, Quebec-Labrador, Canada; The Canadian Mineralogist, v. 53, p. 885–894.

Appendix A2. Site photographs for till and bedrock samples collected in 2015. For site location and information, see Appendix A1.

a)

b)

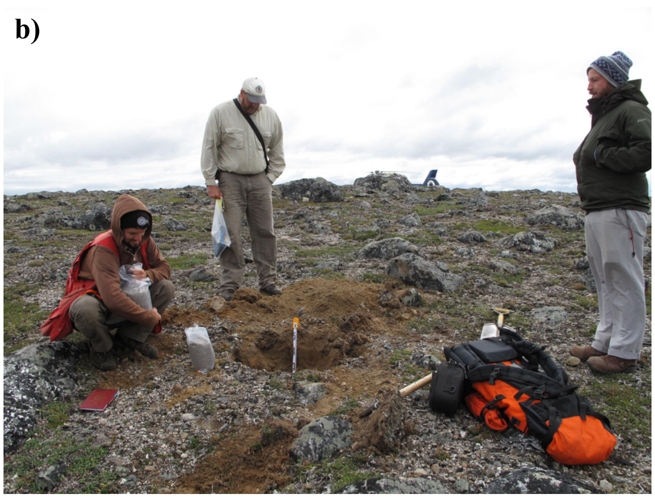

Site 15-MPB-002. Till sample site located 0.25 km up-ice of the Strange Lake intrusion.

Site 15-MPB-003. Bedrock sample site just southeast of the Strange Lake B Zone.

a)

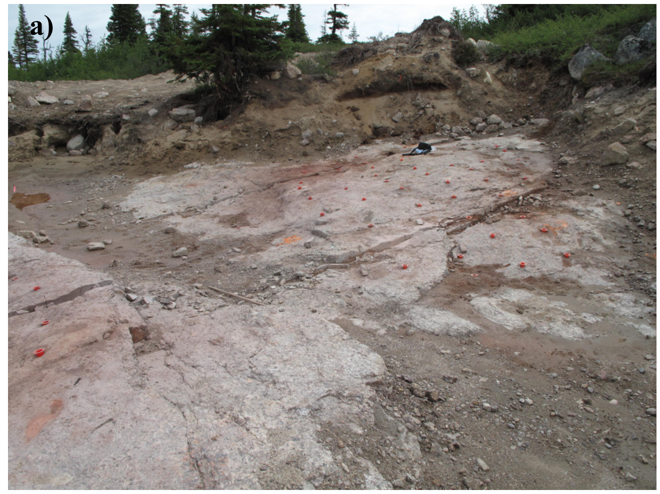

b)

Site 15-MPB-004. Bedrock sample site at the Strange Lake B Zone.

Appendix A2 continued.

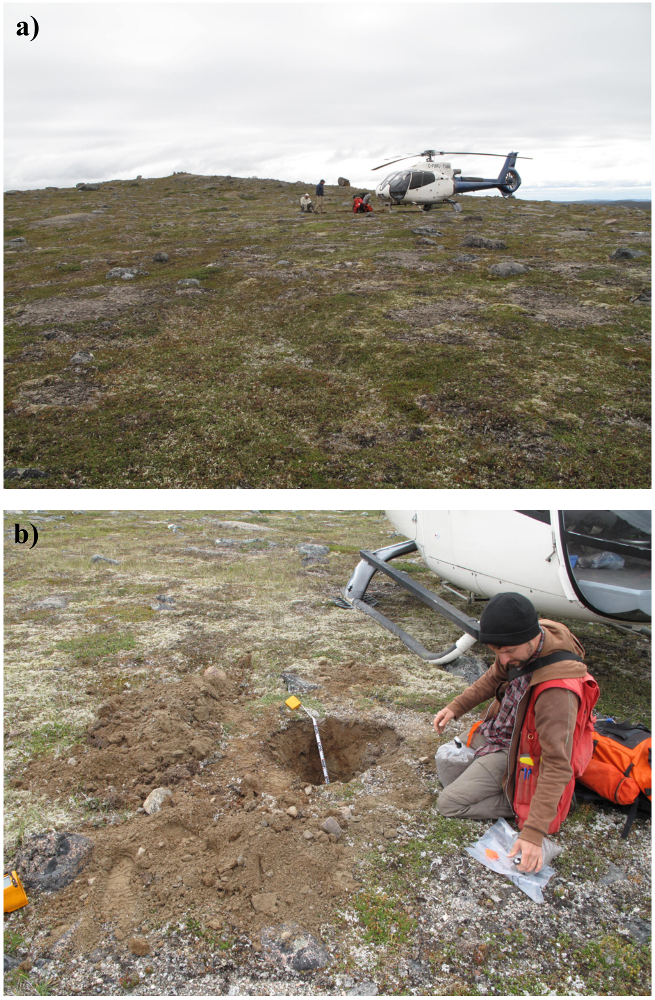

Site 15-MPB-005. Till sample site overlying the Strange Lake intrusion.

Site 15-MPB-006. Till sample site located northeast of the Main Zone.

Site 15-MPB-007. Till sample site overlying the Strange Lake intrusion.

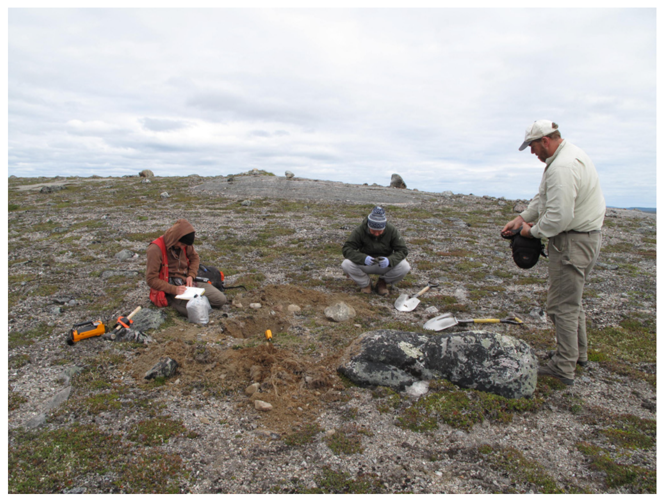

Site 15-MPB-008. Till sample site located 16 km down-ice of the Strange Lake intrusion.

Appendix A2 continued.

Site 15-MPB-009. Till sample site located 50 km down-ice of the Strange Lake intrusion.

Site 15-MPB-010. Till sample site located 27 km down-ice of the Strange Lake intrusion.

Appendix B1. Photographs of polished bedrock slabs of samples collected in 2008. For site location and information, see Appendix A1.

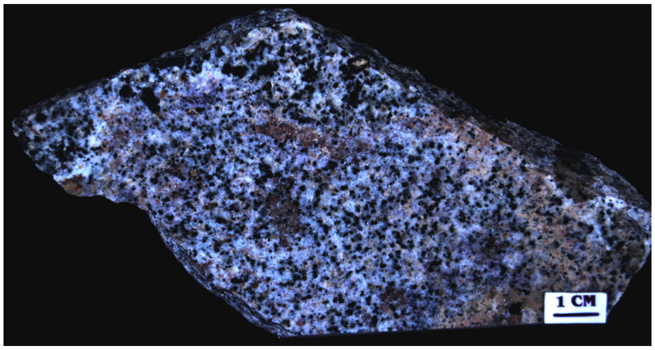

Site 08-MPB-027. Bedrock sample of the Strange Lake Main Zone (formerly the A Zone).

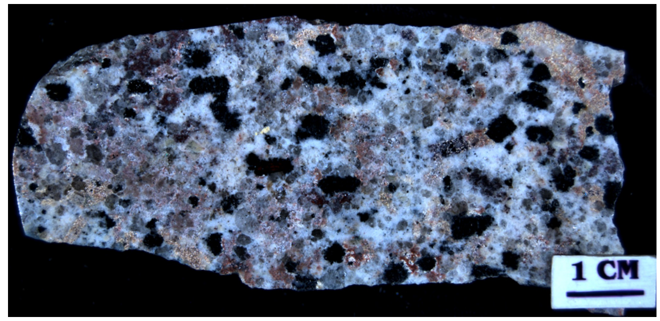

Site 08-MPB-030. Bedrock sample of the Strange Lake Main Zone (formerly the A Zone).

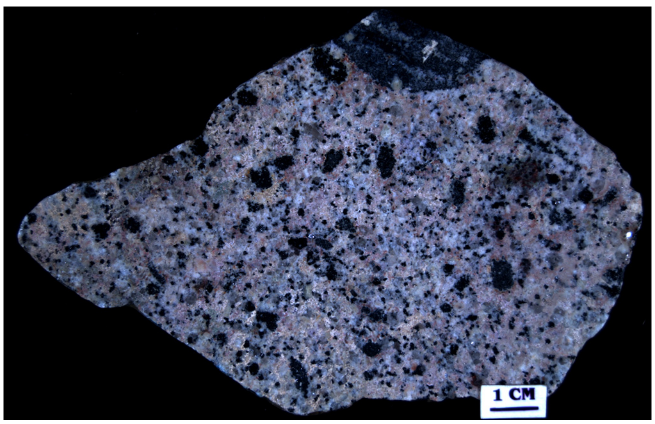

Site 08-MPB-028. Bedrock sample of the Strange Lake Main Zone (formerly the A Zone).

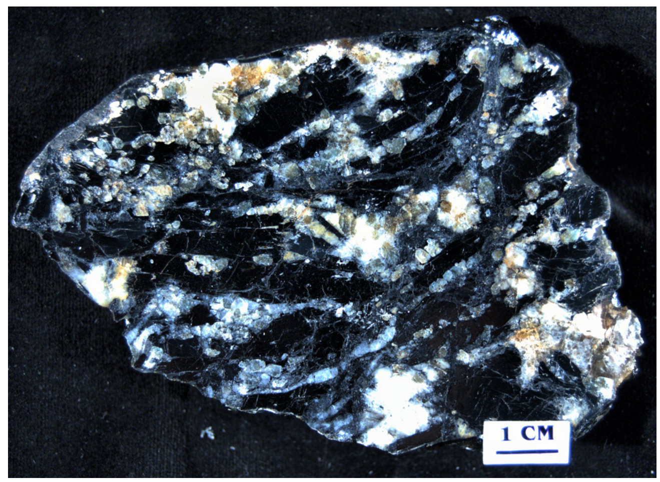

Site 08-MPB-031. Bedrock sample of the Strange Lake Main Zone (formerly the A Zone).

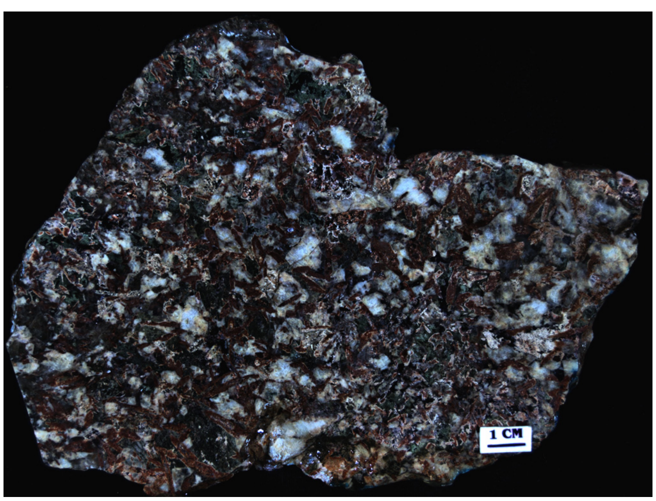

Site 08-MPB-029. Bedrock sample of the Strange Lake Main Zone (formerly the A Zone).

Appendix B2. Binocular microscope descriptions of bedrock hand samples collected in 2008.

by S.A. Averill, Overburden Drilling Management

Sample 08-MPB-027 ARFVEDSONITE GRANITE: Average arfvedsonite (S.G. 3.4) content is higher (10%) than in I. Kjarsgaard's polished section (3%) from a more leucocratic phase of the sample and will produce a large heavy mineral concentrate. Grain size of principal (10%) heavy REE mineral, gittinsite (S.G. 3.6), is 0.5–2 mm and grain size of fluorite averages 0.5 mm. Trace arsenopyrite. Sample is partly coated with lacquer.

Sample 08-MPB-028 ARFVEDSONITE-BIOTITE GRANITE: Arfvedsonite is restricted to subordinate zones and averages only 2% but its grain size ranges up to 5 mm. Main heavy REE mineral, gittinsite, is fine-grained (mostly 0.1–0.2 mm; maximum 0.5 mm) and is similarly restricted, averaging 0.1% versus 10% in I. Kjargaard's section. Trace pyrite. Sample is partly coated with lacquer.

Sample 08-MPB-029 ARFVEDSONITE-AEGIRINE GRANITE: Pegmatitic; all minerals are very coarse- grained (1–10 mm). Abundant heavy aegirine (5%; S.G. 3.6) and gittensite (10%) will produce an oversized HMC; therefore sample should be split before processing. Other major REE minerals (elpidite and catapleiite; 40% combined) are low-density species (S.G. 2.5-2.8). Sample is partly coated with lacquer.

Sample 08-MPB-030 ARFVEDSONITE GRANITE: The grain size of the three main heavy minerals, arfvedsonite (5%), gittinsite (10%) and flourite (2%) overall; less in I. Kjargaard's section, ranges up to 5 mm but their effective grain size is 0.2–0.5 mm due to abundant quartz and feldspar inclusions. Sample is coated with lacquer over a white paint label.

Sample 08-MPB-031 BIOTITE TONALITE: Pegmatitic. Grain size of principal (20%) heavy mineral (apatite) is 1–5 mm. Sample is heavily coated with lacquer and labeled with red marker; some feldspar has been stained blue.

Appendix B3. Petrographic descriptions of bedrock samples collected in 2008.

By I.M. Kjarsgaard, Mineralogical Consultant.

SAMPLE 08-MPB-027

Description: alkali-granite with quartz, perthite and fine-grained elongate albite intergrown with deep blue-green arfvedsonite and pseudomorphs of brown gittinsite + UM2 + quartz ± fluorite after a coarse-grained primary tabular mineral (feldspar ?).

Quartz (20%) medium-grained anhedral rounded grains intergrown with feldspar and amphibole

Perthite (20%) medium-grained subhedral tabular rounded, slightly altered

Albite (15%) fine-grained euhedral elongate tabular grains with multiple twinning piercing quartz and amphibole

Arfvedsonite (3%) medium-grained anhedral deep dark blue-green to olive pleochroic, interstitial to quartz and feldspar.

Gittinsite (10 %) light brown, fine-grained dendritic branching aggregates in pseudomorphs together with quartz; 1st order interference colour, medium high relief nucleating around UM2

Unknown Mineral UM2 (2%) various shades from pale brown to deep red-brown concentrically zoned colloform aggregates intergrown with gittinsite and quartz in pseudomorphs; very high relief, medium to high interference colour

Fluorite (trace) colourless to deep violet together with gittinsite and UM2 in pseudomorphs and interstitial to quartz and feldspar

Hematite (trace) opaque anhedral with reddish FeOOH alteration around rim; white reflectance; also as tiny round aggregates in UM2

Pyrochlore (trace) fine-grained high-relief euhedral yellow to olive-brown zoned octahedra

Apatite (trace) fine- to medium-grained prismatic subhedral rounded grains piercing quartz and feldspar

Titanite (trace) remnants in tabular pseudomorph

Monazite (trace) small euhedral included in arfvedsonite

Microprobe analysis locations on polished thin section:

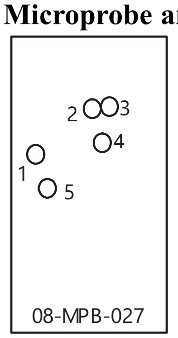

1) titanite in tabular pseudomorph surrounded by feldspar
2) gittinsite and UM2 colloform titanite intergrown with quartz and feldspar
3) gittinsite nucleating around deep red UM2 (?) intergrown with feldspar
4) UM2 (?) intergrown with fluorite in tabular pseudomorph; and opaque dots in fuzzy brown masses of UM2 (?)
5) two euhedral pyrochlore in quartz-feldspar with dark granular masses intergrown with fluorite and ?

Note: UM2 is an unidentified Ca-Fe-Zr-silicate

Appendix B3 continued.

Sample 08-MPB-027 continued

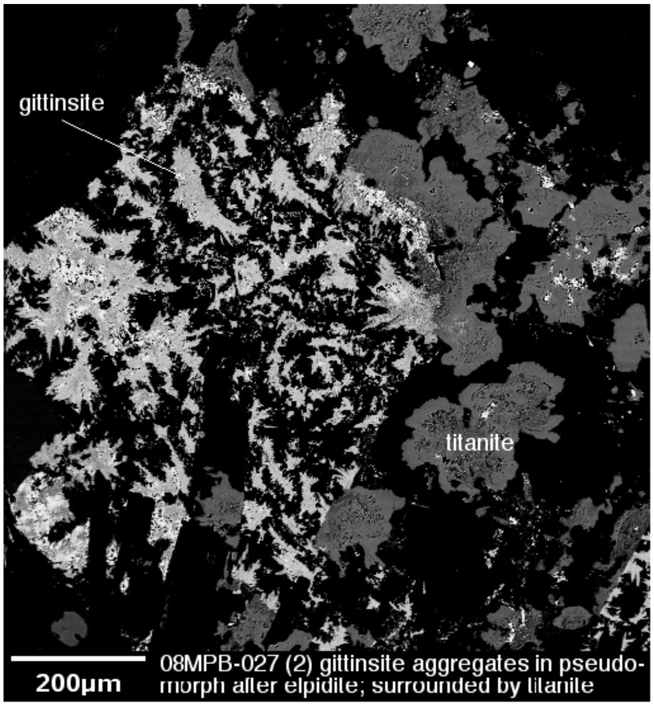

SAMPLE 08-MPB-028

Description: similar to 08-MPB-027 but coarser and with more perthitic feldspar, less albite and more abundant pseudomorphs.

Quartz (25%) medium- to coarse-grained anhedral, rounded grains intergrown with feldspar and amphibole

Perthite (25%) medium- to coarse-grained, subhedral, tabular, rounded, slightly altered

Albite (5%) fine- to medium-grained, euhedral, elongate, tabular grains with multiple twinning piercing quartz and amphibole

Arfvedsonite (4%) medium- to coarse-grained, anhedral, deep dark blue-green to olive, pleochroic, interstitial to quartz and feldspar

Gittinsite (10 %) light brown, fine-grained dendritic branching aggregates in pseudomorphs together with quartz nucleating around UM2; 1st order interference colour, medium-high relief

Unknown mineral UM2 (2%) concentrically zoned colloform aggregates in various shades from pale brown to deep red-brown and black, intergrown with gittinsite; high relief, high interference colour

Fluorite (trace) *Primary*: medium-grained colourless, medium-high relief, knobby chagrin, isotropic, euhedral (8-sided) rounded to anhedral grains intergrown with quartz/feldspar, abundant round inclusions in core; intergrown with arfvedsonite and quartz; octahedral #. *Secondary*: colourless to deep violet; filling voids, together with gittinsite and UM2 in pseudomorphs and interstitial to quartz and feldspar

Hematite (trace) opaque anhedral with reddish FeOOH alteration around rim; white reflectance; also as tiny round aggregates in UM2

Pyrochlore (trace) fine-grained high-relief euhedral greenish yellow to olive-brown zoned octahedra

Apatite (trace) fine- to medium-grained, prismatic, subhedral, rounded grains piercing quartz and feldspar

Titanite (trace) fibrous, light brown aggregates, high relief, high interference colour, intergrown with fluorite and quartz/feldspar

Appendix B3 continued.

Sample 08-MPB-028 continued

Microprobe analysis locations on polished thin section:

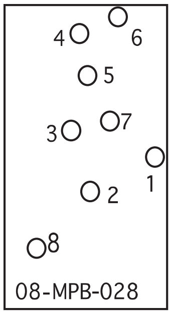

1) fluorite with quartz and opaques
2) titanite with fluorite in quartz + feldspar
3) fluorite and gittinsite intergrown with arfvedsonite
4) titanite replacing arfvedsonite
5) arfvedsonite intergrown with fluorite, UM5, and feldspar
6) euhedral pyrochlores in feldspar matrix
7) colloform UM2 aggregates rimmed by ? (high reflectance)
8) titanite aggregates in quartz/feldspar

SAMPLE 08-MPB-029

Description: coarse (subsolvus ?) alkaligranite with coarse microcline feldspar, abundant reddish brown boat shaped pseudomorphs (after elpidite), aegirine replacing arfvedsonite and cavities filled with secondary violet fluorite.

Quartz (15%) medium- to coarse-grained, anhedral, rounded grains intergrown with feldspar and amphibole

Microcline (25%) coarse, euhedral to subhedral, blocky grains, slightly blotchy and altered and as colourless, medium-grained, euhedral, elongate, tabular grains in parallel aggregates, some deformed (bent), low1st order interference colour (plagioclase ??)

Albite (trace) small subhedral grains in coarse K-feldspar

Arfvedsonite (trace) medium- to coarse-grained, anhedral, deep dark blue-green to olive pleochroic, interstitial to quartz and feldspar.

Aegirine (5%) yellow-green to green, pleochroic, high relief, subhedral to anhedral, replacing arfvedsonite, and itself being replaced by quartz

Gittinsite (10 %) light brown, fine-grained, dendritic branching aggregates in pseudomorphs together with quartz nucleating around UM2; 1st order interference colour, medium-high relief

Unknown Mineral UM2 (2%) various shades from pale brown to deep red-brown, concentrically zoned colloform aggregates intergrown with gittinsite; very high relief, interference colour cannot be assessed because absorption colour too strong

Ca-catapleiite (%) very dark brown to opaque, replacing (?) gittinsite in pseudomorphs (same habit)

Fluorite (trace) colourless to deep violet, concentrically zoned; filling voids, together with gittinsite and UM2 in pseudomorphs and interstitial to quartz and feldspar

Hematite (trace) opaque anhedral with reddish FeOOH alteration around rim; white reflectance; also as tiny round aggregates in UM2

Thorianite (trace) anhedral, opaque, medium-grained rhombic grains or pseudomorphs surrounded by hematite

Pyrochlore (trace) fine- to medium-grained, high-relief, euhedral, greenish yellow to red-brown zoned octahedra

Apatite (trace) fine- to medium-grained prismatic subhedral rounded grains piercing quartz and feldspar

Titanite (trace) fibrous to sparry, light brown aggregates, high relief, high interference colour (carbonate/titanite ?), intergrown with fluorite and quartz/feldspar

Unknown Mineral UM5 (trace) colourless, relief slightly higher than feldspar, good #, low interference colour

Appendix B3 continued.

Sample 08-MPB-029 continued

Microprobe analysis locations on polished thin section:

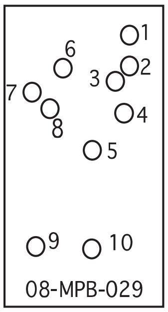

1) two medium-grained euhedral zoned pyrochlore grains at edge of elpidite pseudomorph rimmed by fluorite adjacent to altered feldspar with inclusions of ?
2) fluorite interstitial to deformed laths of K-feldspar; fluorite rimming a colloform aggregates of UM2
3) abundant small pyrochlore octahedra in altered K-feldspar and fluorite intergrown with UM2
4) Titanite as "fibrous" and sparry aggregates in quartz rimmed by fluorite against K-feldspar
5) Ca-catapleiite replacing gittinsite in pseudomorph; tiny pyrochlore octahedra in K-feldspar
6) gittinsite and quartz in pseudomorphs and thorianite rimmed by UM2 intergrown with fluorite
7) three medium-grained pyrochlores in quartz and swirling aggregates of UM9 with interstitial fluorite
8) aegirine replacing arfvedsonite dotted by small opaques; check opaque inclusion in arfvedsonite
9) abundant small pyrochlore grains and UM2 aggregate in altered K-feldspar
10) fluorite, quartz, and various unknown phases in the replacement of aegirine

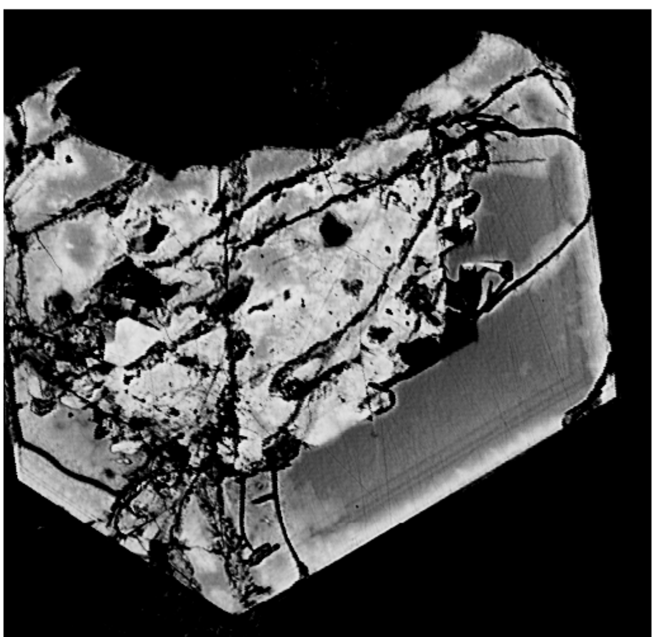

08MPB-029 (1) zoned pyrochlore with altered (metamict?) Nb-rich core

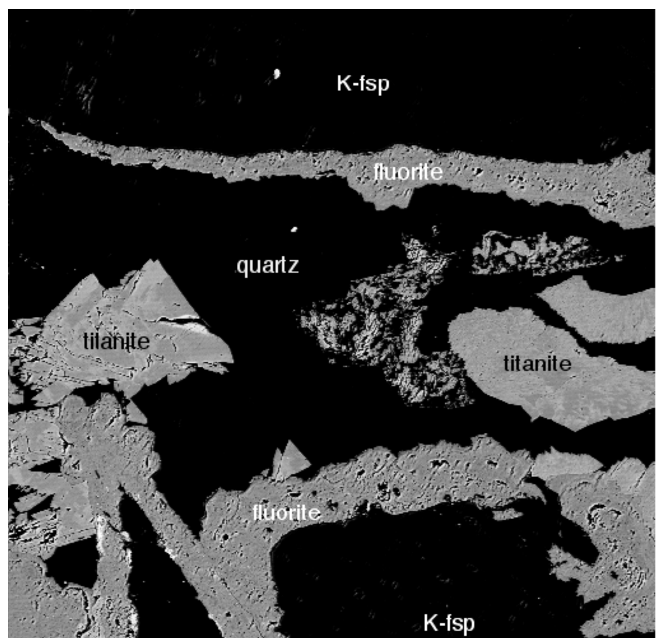

08MPB-029 (4) titanite aggregates in quartz rimmed by fluorite; brighter titanite is Nb-rich

Appendix B3 continued.

Sample 08-MPB-029 continued.

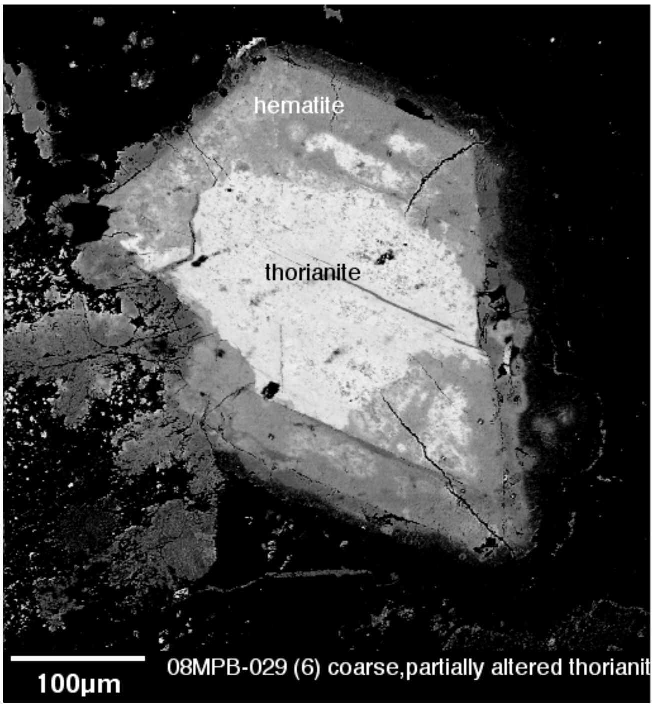

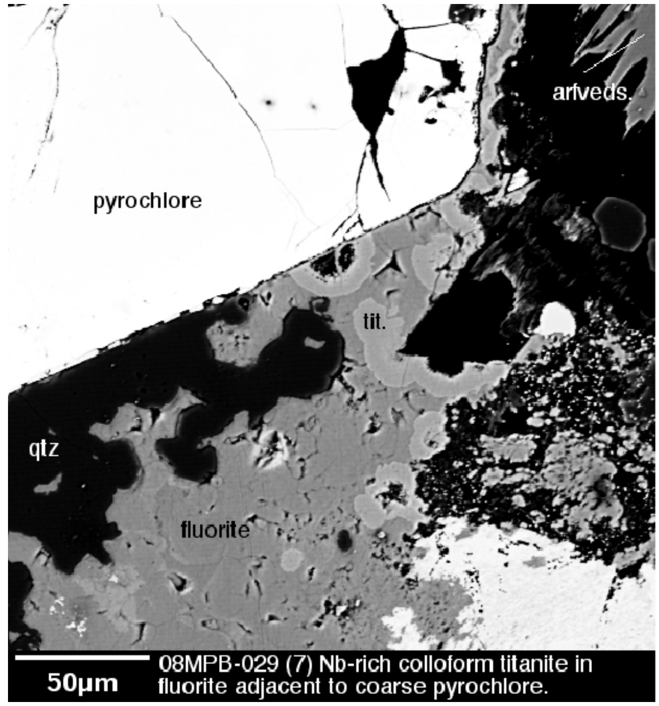

SAMPLE 08-MPB-030

Description: alkaligranite with coarse blue-green arfvedsonite intergrown with quartz, perthite and fine-grained elongate albite. Interstitial pseudomorphs of brown gittinsite + quartz and opaque spiky mineral, trace pyrochlore, and secondary Zr-minerals.

Quartz (20%) medium-grained anhedral rounded grains intergrown with feldspar and amphibole

Perthite (20%) medium-grained subhedral tabular rounded, slightly altered

Albite (15%) fine-grained, euhedral, elongate tabular grains with multiple twinning piercing quartz and amphibole

Arfvedsonite (3%) medium-grained, anhedral, deep dark blue-green to olive, pleochroic, interstitial to quartz and feldspar.

Gittinsite (10 %) light brown, fine-grained, dendritic branching aggregates in pseudomorphs together with quartz; 1st order interference colour, medium-high relief nucleating around UM2

Unknown Mineral UM2 (2%) various shades from pale brown to deep red-brown concentrically zoned colloform aggregates intergrown with gittinsite and quartz in pseudomorphs; very high relief, interference colour cannot be assessed because absorption colour too strong

Fluorite (trace) colourless, anhedral grains in arfvedsonite or interstitial to quartz and feldspar

Hematite (trace) opaque anhedral with reddish FeOOH alteration around rim; white reflectance; also as tiny round aggregates in UM2

Pyrochlore (trace) fine-grained, high-relief, euhedral, yellow to olive-brown zoned octahedra

Titanite (trace) fibrous, light brown aggregates, high relief, high interference colour, intergrown with fluorite and quartz/feldspar

Unknown Mineral UM9 reddish brown, high relief, oriented inclusions in arfvedsonite

Appendix B3 continued.

Sample 08-MPB-030 continued.

Microprobe analysis locations on polished thin section:

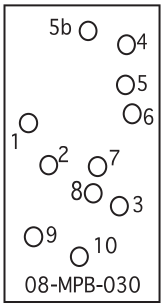

1) albite and oriented inclusions of UM9 in arfvedsonite surrounded by K-feldspar; what are stepped grains in K-feldspar
2) gittinsite and opaque in pseudomorph interstitial to arfvedsonite, quartz and plagioclase.
3) high relief, brown, translucent mineral interstitial to plagioclase and K-feldspar
4) arfvedsonite with fluorite inclusion surrounded by albite laths and UM2 aggregates, minor unknown opaque and brown alteration between quartz grains.
5) fine-grained radial aggregate of ? in radiating dendritic aggregates of gittinsite dotted with opaques
6) deep brown to black, spiky aggregates intergrown with or replacing gittinsite interstitial to quartz-feldspar; small pyrochlore at rim of circle
7) intense emerald-green aggregates associated with fluorite surrounding albite
8) granular, high relief, colourless mineral intergrown with fluorite in pseudomorph
9) high relief, high interference colour, fibrous aggregates (titanite?) in shades of light brown interstitial to albite and quartz.
10) radiating rounded aggregates of high relief, medium interference colour, mineral (secondary zircon ?) and small cubes of colourless, low interference colour mineral in quartz intergrown with gittinsite
11) colourless micaceous minerals in void adjacent to anhedral brandy-coloured mineral in quartz-feldspar

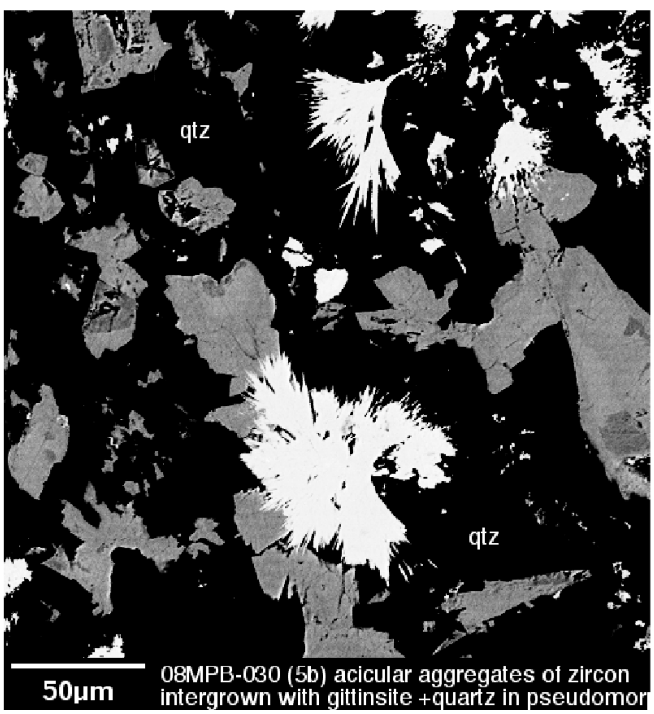

Appendix B3 continued.

SAMPLE 08-MPB-031

Description: abundant, coarse, olive-brown biotite intergrown with coarse, rounded apatite, feldspar, and quartz.

Biotite (66%) very coarse, dark khaki, slightly deformed and kinked, fine-grained around edges

Apatite (20%) coarse, colourless, euhedral to subhedral, rounded grain with tiny elongate inclusions parallel c-axis, fractured and veined; slightly higher relief than feldspar and quartz

Feldspar (6%) coarse rounded grains; fine, granular cementing coarser grains

Quartz (8%) medium-grained granoblastic matrix

Uraninite (trace) fine-grained, euhedral, orange-red grains causing bleached halos in biotite, partially dissolved; isotropic or metamict

Rutile (trace) tiny euhedral flakes embedded in biotite

Zircon (trace) euhedral elongate prismatic grains, strongly zoned, associated with patite and pyrochlore

Muscovite (trace) inclusions in apatite

Microprobe analysis locations on polished thin section:

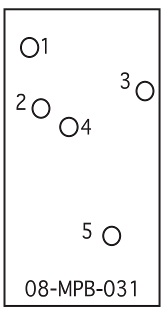

1) orange-red octahedra in coarse biotite and associated with zircon in quartz
2) coarse apatite in fine-grained biotite
3) clinozoisite ? rimming biotite against apatite, various other inclusions in apatite
4) zircon intergrown with apatite
5) two opaque grains in coarse biotite

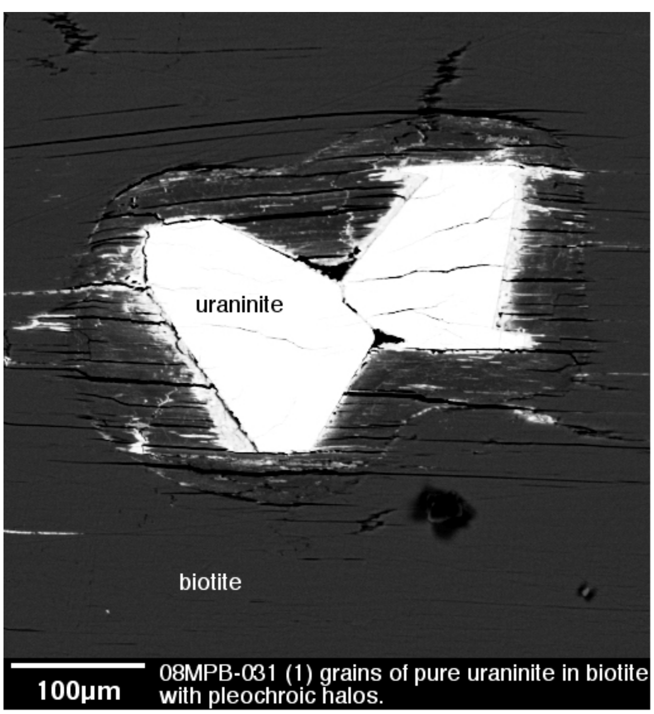

08MPB-031 (1) grains of pure uraninite in biotite with pleochroic halos.

Appendix B3 continued.

SAMPLE 08-MPB-032

Description: subsolvus granite with quartz, albite, and K-feldspar intergrown with abundant oriented pseudomorphs (1) gittinsite + quartz after elpidite, (2) UM9 replacing arfvedsonite, and (3) UM2 + quartz + fluorite replacing elongate rectangular grains.

Quartz (15%) medium- to coarse-grained, anhedral grains interstitial to K-feldspar and enclosing albite

Microcline (25%) medium-grained, subhedral, blocky grains (euhedral in amphibole), slightly blotchy and altered

Albite (25%) abundant fine-grained elongate, slightly rounded grains

Arfvedsonite (5%) medium- to coarse-grained anhedral, deep dark olive-green to black, intergrown with albite, replaced by aegirine and UM9

Unknown Mineral UM9 (1%) yellow to reddish brown, acicular aggregates replacing arfvedsonite

Aegirine (5%) yellow-green to green pleochroic, high relief, subhedral to anhedral, replacing arfvedsonite, and itself being replaced by quartz

Gittinsite (20%) light brown, fine-grained dendritic branching aggregates in pseudomorphs together with quartz nucleating around UM2; 1st order interference colour, medium-high relief

Unknown Mineral UM2 (5%) various shades from pale brown to deep red-brown, concentrically zoned, colloform aggregates; very high relief, medium-high interference colour in rectangular pseudomorphs

Ca-catapleiite (trace) very dark brown to opaque, replacing (?) gittinsite in pseudomorphs (same habit)

Fluorite (trace) colourless to deep violet, concentrically zoned; together with UM2 in rectangular pseudomorphs

Monazite (trace) coarse (!), euhedral, colourless, high-relief mineral, pink interference colour, chagrin

Pyrochlore (trace) fine-grained, euhedral, yellow-green to brown octahedra disseminated in feldspar matrix

Microprobe analysis locations on polished thin section:

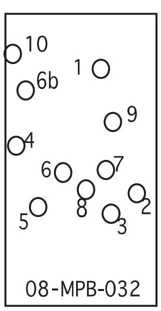

1) coarse euhedral colourless monazite, pink interference colour (UM1), chagrin
2) titanite aggregates with UM2 and pyrochlore interstitial to feldspar and gittinsite
3) yellow-red-brown acicular sheaves of UM3 replacement near opaque amphibole (?)
4) high relief, high interference colour aggregates in quartz-feldspar matrix with pyrochlore, gittinsite in pseudomorph
5) UM2 and quartz + titanite in rectangular pseudomorphs, gittinsite + quartz in elpidite pseudomorph both in quartz-feldspar matrix with pyrochlore
6) What are spiky, colourless, high-relief grains in rectangular pseudomorphs?
7) colloform UM2 intergrown with quartz; gittinsite in pseudomorph and pyrochlore interstitial to feldspar
8) UM1 in quartz-feldspar matrix with aegirine replacing arfvedsonite, gittinsite and UM2 pseudomorphs
9) high relief, acicular, radiating zircon aggregates with gittinsite in pseudomorphs
10) colourless, low interference colour mineral intergrown with fluorite in pocket; various minerals +fluorite in rectangular pseudomorphs; spiky acicular aggregates in elpidite pseudomorph

Appendix B3 continued.

Sample 08-MPB-032 continued.

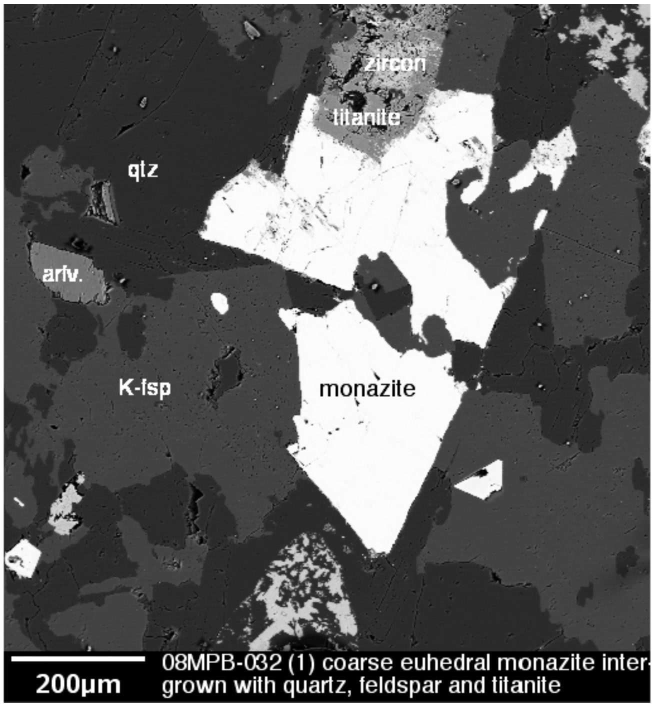

Appendix B4. Photographs of polished bedrock slabs of samples collected in 2015. For site location and information, see Appendix A1.

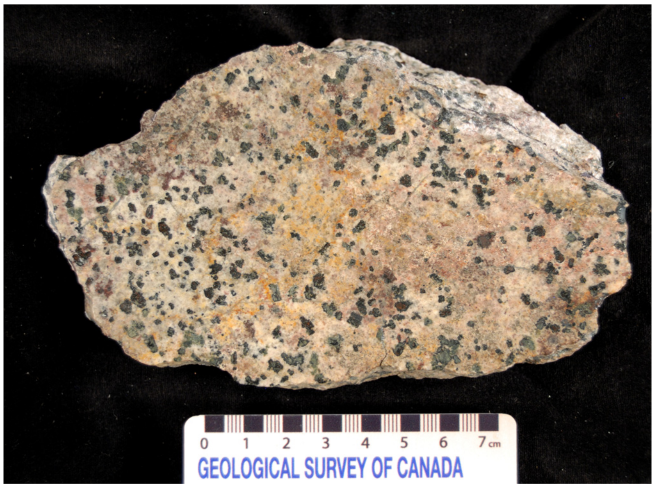

Site 08-MPB-003. Bedrock sample of the Strange Lake B Zone.

Site 08-MPB-006. Bedrock sample of the Strange Lake Main Zone (formerly the A Zone).

Site 08-MPB-004A-2. Bedrock sample of the Strange Lake B Zone.

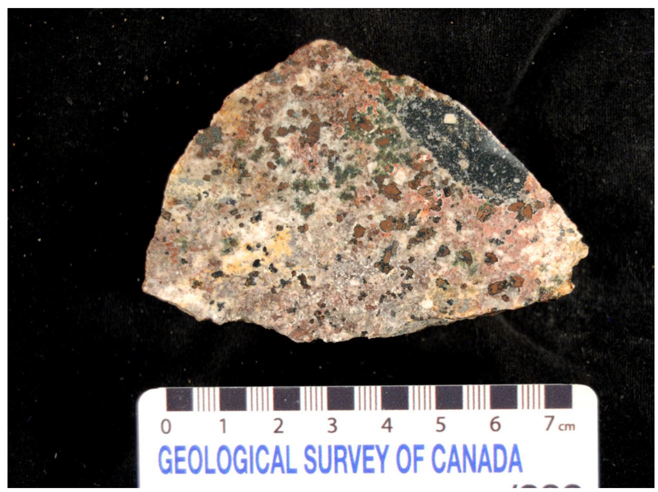

Site 08-MPB-010A. Cobble collected 35 km down-ice (east-northeast) of the Strange Lake deposit.

Site 08-MPB-004. Bedrock sample of the Strange Lake B Zone.

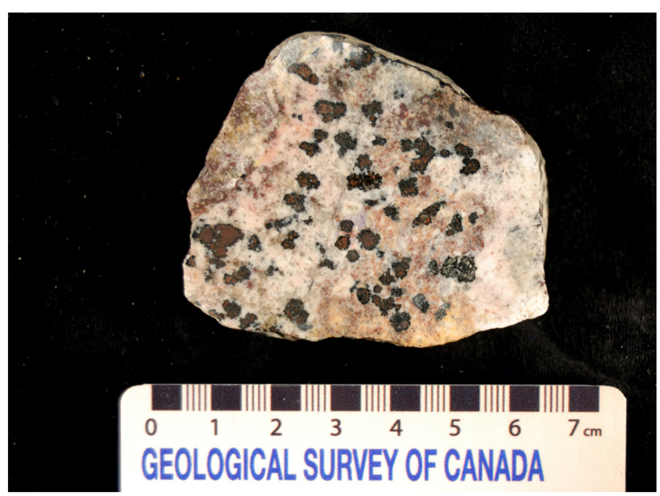

Site 08-MPB-010B. Cobble collected 35 km down-ice (east-northeast) of the Strange Lake deposit.

Appendix B5. Binocular microscope descriptions of bedrock hand samples collected in 2015.

by S.A. Averill, Overburden Drilling Management

Sample 15-MPB-003 PORPHYRITIC ALKALI MICROGRANITE: Single, sawn slab. Pale pink (hematite-stained) to rusty red, massive, nonmagnetic, mafic-phyric plutonic rock consisting of 15% coarse (3–5 mm), green aegirine (SEM-confirmed) phenocrysts rimmed by black arfvedsonite (SEM-confirmed) in a fine-grained, micro-granitic (0.3–0.5 mm) groundmass composed of 60% white K-feldspar (SEM-confirmed), 30% quartz, and 10% REE minerals (soft, white; mainly armstrongite, elpidite, and ferriallanite; SEM confirmed) as 0.1–0.3 mm grains intergrown with similarly fine-grained feldspar and quartz in irregular, 3–5 mm patches. Fractures in rock contain 1% hematite as an earthy, brick-red film.

Sample 15-MPB-004A-02 GRAPHIC ALKALI GRANITE: Single sawn slab. Mottled white (but mostly hematite-stained red-orange) and dark green, massive, nonmagnetic plutonic consisting of coarse-grained (5–8 mm), euhedral to graphically intergrown green aegirine (20%; locally rimmed by fine-grained black arfvedsonite), K-feldspar (30%, SEM-confirmed) and quartz (30%), 20% slightly smaller (2–5 mm), pale grey, euhedral, wedge-shaped crystals of zircon (SEM-confirmed) and 3% dark purple fluorite as 0.1–0.5 mm crystals graphically intergrown with the silicate minerals.

Sample 15-MPB-004B LEUCOGRANITE MAGMATIC BRECCIA: Single sawn specimen. Main phase comprising 60% of sample is a pink, massive, nonmagnetic, varitextured plutonic rock consisting of closely packed, euhedral to polygonal grains of K-feldspar with 15% interstitial quartz and no mafic minerals. Above phase evidently formed as a crystal mush within a hydrous melt as it occurs in chaotic patches separated by large (5–10 mm), amoeboid zones that constitute 40% of the rock and variably consist of quartz (20%), pale brown to dark purple-black fluorite (5%; SEM confirmed) and open vugs (15%) that were probably once occupied by calcite and have been partly refilled by pink aggregates (10%) of drusy silica (SEM-confirmed) and a white powder consisting of minute (1–3 μm), apparently supergene zircon crystals (also SEM-confirmed), or by specular hematite (2%).

Sample 15-MPB-006 VEINED TONALITE: Two fist-sized hand specimens. White, black-flecked, massive, nonmagnetic, equigranular plutonic rock consisting of medium-grained (0.7–1.5 mm) hornblende (20%), subhedral, albite-twinned plagioclase (60%), and quartz (20%) with trace leucoxene. Tonalite is cut by a 1 cm-wide vein with a core of massive, colourless quartz bordered by coarse-grained (2–5 mm) augite (SEM-confirmed) that ranges from nearly colourless to the characteristic pale emerald-green of low-Cr diopside. Vein has a 1 cm-wide selvage of very fine-grained (0.1–0.3 mm), hornfelsed tonalite.

Sample 15-MPB-010A PORPHYRITIC ALKALI MICROGRANITE: Sawn, fist-sized specimen from rounded boulder. White to pale pink (hematite-stained), prominently flecked bright green, black, and rusty brown, massive, nonmagnetic, strongly mafic-phyric plutonic rock consisting of 5% bright green, 2–5 mm aegirine (SEM-confirmed) phenocrysts and 15% dark blue-black to rusty brown (limonite-stained along cleavage planes), similar-sized, arfvedsonite (SEM-confirmed) phenocrysts in a finer grained, 0.3–0.5 mm groundmass of anhedral grains of K-feldspar (60%; SEM-confirmed) and quartz (35%), with 3% white to yellow to red-brown (iron-stained) leucoxene (SEM-confirmed) as small, 0.1–0.3 mm grains aggregated with quartz, feldspar, apatite, and minor purple fluorite (0.1% of sample) in larger (1–5 mm), irregular patches.

Appendix B6. Petrographic descriptions of bedrock samples collected in 2015.

By I.M. Kjarsgaard, Mineralogical Consultant.

SAMPLE 15-MPB-003 alkaline granite

Description: medium-grained, subhedral yellow-green aegirine is overgrown (or partially replaced) by very dark blue-green arfvedsonite, which in turn contains inclusions of small tabular plagioclase crystals that are also scattered throughout the section and form aggregates interstitial to and intergrown with quartz and microcline. Some of the amphibole contains dark brown streaks that appears to be an alteration, although composition does not show much difference from regular arfvedsoneite (possibly just oxidized). Other red-brown minerals (allanite and an unidentified Zr-Ca-Y-silicate) fill interstices between blocky feldspar. Coarser euhedral microcline is more altered than the finer grained albite and quartz appears to be both primary and secondary (hydrothermal). Primary euhedral, olive greenish pyrochlore crystals show sharp euhedral outlines but abundant inclusions and internal resorption features. It is typically intergrown with the outer areas of arfvedsonite. Some areas show euhedral outlines filled with a fine granular high-relief mineral (UM1) and fine-grained brown acicular aggregates of an another unidentified Zr-silicate (UM2) intergrown with albite and quartz, all replacing what probably was primary elpidite. There are other areas in the thin section where the original mineral assemblage appears to have been dissolved leaving behind voids that are now filled with violet to clear zoned fluorite and a very fine-grained orange-brown globular mineral (UM3: Zr-Y-silicate) that in some cases shows Fe-staining.

Quartz (25%) medium- to coarse-grained, anhedral, intergrown with feldspar, some show inclusions trails (i.e. could be of hydrothermal origin)

Microcline (5%) blocky, euhedral, medium-sized crystal with tartan twinning and greyish due to alteration

Albite (40%) fine- to medium-grained, euhedral, intergrown with quartz, microcline, and amphibole

Aegirine (9%) yellowish green, pleochroic, anhedral, medium-grained, blocky cores in arfvedsonite, with 88° cleavage, high relief, and high interference colour

Arfvedsonite (16%) from deep inky blue to olive-brown, pleochroic, coarse, subhedral to euhedral overgrowing and incorporating partially resorbed aegirine crystals; with red-brown, streaky alteration

Pyrochlore (trace) fine-grained, sharply euhedral, olive-green, isotropic trapezoidal crystals with big holes and slight zonation

Allanite (0.5%) clear reddish brown to brown, anhedral, fractured grains interstitial to feldspar

Unknown Mineral UM1 (Zr-Y-RE-silicate) (1%) very fine-grained, high-relief, colourless granular to lace-like aggregates in pseudomorphs after elpidite

Unknown Mineral UM2 (Zr-Ca-Y-silicate) (1%) fine-grained, light brown to reddish brown, acicular aggregates in euhedral pseudomorphs after elpidite?

Fluorite (trace) fine-grained, euhedral to anhedral in voids/dissolved areas in quartz-feldspar matrix associated with globular mineral

Unknown Mineral UM3 (Zr-Y-RE-silicate) (trace) very fine-grained, globular orange-brown, translucent, high-relief aggregates in voids associated with fluorite

Hematite (trace) minor rusty to black staining in and around Fe-silicates (aegririn, arfvedsonite) and in secondary Zr-silicates

Titanite (trace) anhedral, very high relief, high interference colour intergrown with aegirine

Microprobe analysis locations on polished thin section:

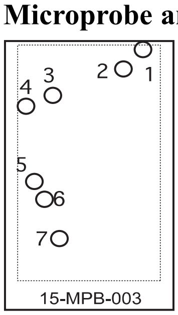

1) two medium-grained euhedral zoned pyrochlore grains at edge of elpidite pseudomorph rimmed by fluorite adjacent to altered feldspar with inclusions of ?
2) fluorite interstitial to deformed laths of K-feldspar; fluorite rimming a colloform aggregates of UM2
3) abundant small pyrochlore octahedra in altered K-feldspar and fluorite intergrown with UM2
4) Titanite as “fibrous” and sparry aggregates in quartz rimmed by fluorite against K-feldspar

Appendix B6 continued.

Sample 15-MPB-003 continued.

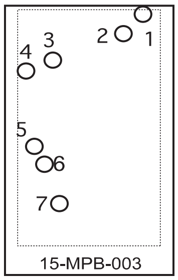

5) Ca-catapleiite replacing gittinsite in pseudomorph; tiny pyrochlore octahedra in K-feldspar
6) gittinsite and quartz in pseudomorphs and thorianite rimmed by UM2 intergrown with fluorite
7) three medium-grained pyrochlores in quartz and swirling aggregates of UM9 with interstitial fluorite
8) aegirine replacing arfvedsonite dotted by small opaques; check opaque inclusion in arfvedsonite
9) abundant small pyrochlore grains and UM2 aggregate in altered K-feldspar
10) fluorite, quartz, and various unknown phases in the replacement of aegirine

SAMPLE 15-MPB-004A-2 metasomatically altered alkaline granite

Description: medium-grained alkali granite with extensive replacement of its primary mineral assemblage. Primary textures are still preserved in the form of euhedral grain outlines. A sharply euhedral elongate prismatic mineral (elpidite?) up to 7.5 mm in length has been replaced by quartz±feldspar and very fine-grained, high-relief aggregates of secondary Zr-minerals (UM1). They are stained reddish brown by hematite and are intergrown with coarse euhedral aegirine that has been partially replaced by quartz and dark red-brown arfvesonite ± pale anhedral titanite. In the quartz matrix are ghosts of a third mineral with almost invisible (but sharply euhedral) outline containing thorite grains surrounded by dark fission tracks. Interstitial to the primary euhedral phases are large irregular areas of a light brown mineral (hematite-stained kalonite-altered feldspar) intergrown with abundant clear to deep violet zoned fluorite enclosing abundant holes. The entire rock has been infused with medium-grained hydrothermal quartz, with grain boundaries that transcend those of the primary minerals. One of the few primary minerals left intact is zoned olive-green pyrochlore, which occurs as small sharply euhedral trapezoidal grains and aggregates throughout the assemblage.

Quartz (30%) medium- to coarse-grained, anhedral intergrown with feldspar, some show inclusions trails (i.e. could be of hydrothermal origin)

Feldspar (20%) medium-grained, blocky, euhedral with Carlsbad twinning, heavily altered by reddish brown fuzzy mineral (kaolinite±hematite?) and fluorite

Aegirine (20%) yellowish green, euhedral, medium- to coarse-grained blocky grains with near-90° cleavage, high relief and high interference colour, partially replaced by quartz, aenigmatite, and titanite

Unknown Mineral UM0 (15%) only euhedral outlines of up to 7.5 mm-long monoclinic crystals remain, the rest is now quartz + secondary Zr-minerals ± hematite

Pyrochlore (trace) fine-grained, sharply euhedral, olive-green, isotropic trapezoidal crystals with slight zonation in quartz matrix

Aenigmatite (1%) dark red-brown, zoned, anhedral in partially dissolved aegirine

Unknown Mineral UM2 (1%) fine-grained, light brown, acicular aggregates in euhedral pseudomorphs after elpidite?

Fluorite (4%) fine-grained, colourless to deep violet, zoned anhedral in voids/dissolved areas intergrown with hematite-stained altered feldspar

Aeschynite [(Y,Ca,Fe)(Ti,Nb)$_2$(O,OH)$_6$] (trace) very fine-grained, globular, orange-brown, translucent aggregates in elpidite pseudomorphs

Thorite [ThSiO$_4$] (trace) small dark brownish (metamict) grains with diffuse outline surrounded by dark fission tracks in quartz

Appendix B6 continued.

Sample 15-MPB-004A-2 continued.

Britholite [$(Ce,Ca,Th,La,Nd)_5(SiO4,PO_4)_3(OH,F)$] (trace) very fine-grained, anhedral aggregates (only detected by microprobe)

Hematite (1%) as fine-grained bladed or colloform aggregates appearing opaque to reddish brown translucent commonly intergrown with altered feldspar and fluorite

Microprobe analysis locations on polished thin section:

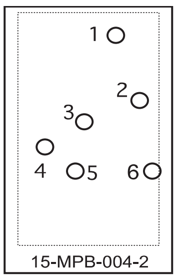

1) several round grains of thorite surrounded by fission tracks and secondary Zr-Th-silicate hematite in quartz - K-feldspar; pyrochlore aggregate at rim (photo 8)
2) round grain of thorite surrounded by fission tracks and hematite in quartz; pyrochlore aggregate at rim, minor fluorite (photo 9)
3) globular aggregates of yellow aeschynite with dark cores (hematite?) in quartz pseudomorph adjacent to kaolinite altered feldspar (photo 5)
4) acicular aggregates of dark translucent mineral in hydrothermal quartz and fine, granular, high-relief UM1, traces of fluorite (photo 6)
5) hematite, fluorite, and a few yellow aeschynite globules in heavily kaolinite-altered feldspar infused by hydrothermal quartz
6) deep brown allanite with euhedral inclusion of fluorite and fine-grained aggregates of aeschynite and UM1 intergrown with titanite and aegirine

SAMPLE 15-MPB-004B metasomatically altered alkaline granite

Description: abundant fresh, fine- to medium-grained, blocky microcline and a few much larger perthitic grains intergrown with coarse hydrothermal quartz. Interstitial to the fresh feldspar are remnants of older, pale brown, highly altered feldspar and dark, heavily altered pseudomorphs of other primary minerals. The "fresh" feldspars have a strange surface texture resembling coarse textile due to abundant, very fine-grained, oriented inclusions (appearing as pits at the surface) and their twin and exsolution lamellae are distorted and fuzzy suggesting they underwent recrystallization of some kind. The dark pseudomorphs consist of very, very fine, granular, high-relief minerals (UM1) stained reddish brown by hematite with discrete grains of fine grained secondary zircon. Fine-grained aggregates of a high-relief mineral also occur in the interstitial altered feldspar. Deep violet fluorite occurs in pockets interstitial to altered feldspar and other pseudomorphs. Fine-grained olive-green trapezoidal grains of pyrochlore are disseminated throughout the microcline-quartz-perthite matrix and another high-relief, barely translucent, isometric mineral with medium-high reflectance occurs in the altered areas.

Quartz (22%) medium- to coarse-grained, anhedral, intergrown with feldspar, some show inclusions trails (i.e. could be of hydrothermal origin)

Feldspar (66%) medium-grained, blocky microcline and larger rounded perthite grains with fuzzy twin and exsolution lamellae and strong surface texture (chagrin); primary feldspar is interstitial and heavily altered by light brown mineral (kaolinite)

Pseudomorphs (10%) filled with very fine, granular, brownish, high-relief aggregates + secondary (fibrous?) zircon

Pyrochlore (trace) fine-grained, sharply euhedral, trapezoidal, olive-green, isotropic crystals with slight zonation in quartz-feldspar

Unknown Mineral UM2 (1%) very fine-grained, light brown, acicular aggregates in primary quartz-feldspar

Aeschynite [$(Y,Ca,Fe)(Ti,Nb)_2(O,OH)_6$] (trace) very fine-grained, globular, orange-brown, translucent aggregates in altered areas

Titanite (trace) fine-grained, pale yellow, anhedral, very high-relief grains in dark pseudomorphs and interstitial to fluorite

Appendix B6 continued.

Sample 15-MPB-004B continued.

Fluorite (1%) fine-grained, colourless to deep violet, zoned, anhedral intergrown with altered feldspar

Zircon (trace) colourless, anhedral, shard-like, high-relief inclusions with medium interference colour in alteration patches (secondary)

Allanite (trace) medium-relief, reddish brown to olive-brown, anhedral grains interstitial to feldspar

Thorite (trace) very fine-grained, isometric, barely translucent, dark grey, high-relief, euhedral grains with high reflectance

Unknown Mineral UM5 (trace) fine-grained, colourless, radial aggregates in elongate patches in hematite-stained UM1 alteration patches/pseudomorphs

Britholite [(Ce,Ca,Th,La,Nd)5(SiO_4,PO_4)$_3$(OH,F)] (trace) very fine-grained anhedral aggregates (only detected by microprobe)

Hematite (trace) fine-grained, bladed or colloform aggregates appearing opaque to reddish brown, translucent, commonly intergrown with altered feldspar and fluorite

Brookite ?[TiO_2] (trace) fine-grained, euhedral, very high-relief, rectangular, brown grain

Microprobe analysis locations on polished thin section:

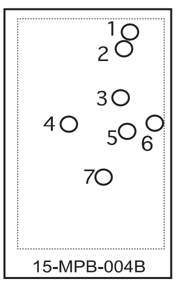

1) secondary zircon in pseudomorph filled with hematite-stained UM1 ± britholite
2) rounded aggregates of UM5 in hematite-stained UM1 (UM5 has same composition as UM1)
3) euhedral pyrochlore and anhedral titanite in kaolinite-altered feldspar
4) rounded aggregates of UM5 in hematite-stained UM1
5) very high-relief, very high-interference colour titanite in dark UM aggregates interstitial to euhedral quartz
6) very high-relief, pale yellow titanite interstitial to euhedral fluorite
7) extremely high-relief, brownish, euhedral grain (TiO_2- brookite??) in quartz, hematite-stained UM in arfvedsonite at outer rim

SAMPLE 15-MPB-006 "fresh" alkaline granite

Description: abundant medium-grained, euhedral to subhedral feldspar (sodic plagioclase, perthitic alkalifeldspar) is intergrown with interstitial anhedral quartz, subhedral yellow-green aegirine intergrown with intense dark blue-green arfvedsonite, and acicular aggregates of fine-grained, brown astrophyllite. Some of the feldspar grains are overprinted by colourless, anhedral muscovite. Euhedral olive greenish pyrochlore crystals and anhedral rounded fluorite with abundant inclusions are intergrown with aegirine-arfvedsonite and quartz-feldspar, respectively; fuzzy round brownish inclusions in feldspar may be a metamict mineral. Traces of hematite stain small areas in feldspar.

Quartz (20%) medium-grained, anhedral intergrown with feldspar

Perthitic microcline (35%) blocky euhedral medium-size crystal with tartan twinning and patchy perthite

Plagioclase (25%) fine- to medium-grained, elongate, euhedral laths intergrown with alkalifeldspar and quartz

Aegirine (8%) yellowish green, medium-grained, anhedral, with abundant round inclusions, intergrown with arfvedsonite

Arfvedsonite (7%) medium-grained, anhedral, deep ink blue to olive-brown, pleochroic, intergrown with aegirine interstitial to feldspar

Astrophyllite (3%) fine grained, yellow-brown, acicular aggregates in and interstitial to feldspar

Pyrochlore (trace) extremely fine-grained, clear to fine-grained, euhedral, olive-green isotropic trapezoidal crystals intergrown with aegirine-arfvedsonite, the smaller ones in quartz/feldspar

Appendix B6 continued.

Sample 15-MPB-006 continued.

Fluorite (trace) fine-grained, anhedral, rounded grains with abundant round inclusions, associated with quartz-feldspar and aegirine

Thorite (trace) fine-grained anhedral fuzzy, brownish, round inclusions in feldspar

Monazite (trace) colourless, clear, anhedral, very high-relief, 3^{rd} order interference colour interstitial to feldspar at rim of section

Unknown Mineral UM1 (trace) fine-grained, granular, colourless, high-relief grains with grey interference colour

Hematite (trace) minor rusty to black staining around Fe-silicates (aegirine/arfvedsonite)

Microprobe analysis locations on polished thin section:

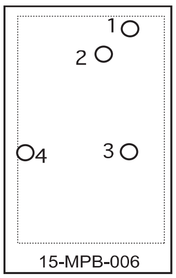

1) monazite with UM1 intergrown with yellow-brown, anhedral allanite and arfvedsonite/aegirine
2) astrophyllite interstitial to K-feldspar and arfvedsonite
3) aegirine intergrown with pyrochlore at rim in quartz-feldspar
4) monazite and fine-grained, dark brown aggregates interstitial to feldspar with arfvedsonite

SAMPLE 15-MPB-010A hydrothermally altered alkaline granite

Description: conspicuous dark euhedral crystals in this section are medium-size grains of dark blue-green arfvedsonite that have been partially to almost totally replaced by a dark red-brown phase and is intergrown with minor aegirine, which is not altered but fractured and partly broken out leaving large voids. These minerals occur in a matrix of fine- to medium-grained, subhedral to euhedral microcline + albite intergrown with quartz, some of which shows inclusions trails and appears to be of hydrothermal origin and possibly replacing some of the feldspar assemblage. Minor violet fluorite and euhedral olive pyrochlore is intergrown with feldspar and/or MgFe-silicates. An unknown colourless mineral with high relief and low interference colour is intergrown with aegirine and feldspar. Towards the lower end of the section, very fine-grained granular and dendritic aggregates of secondary Zr-minerals are intergrown with quartz-feldspar.

Quartz (35%) medium- to coarse-grained, anhedral, with inclusion trails, intergrown with and replacing feldspar

Perthitic microcline (10%) blocky euhedral medium-size crystal with tartan twinning and patchy perthite

Plagioclase (25%) fine- to medium-grained elongate euhedral laths intergrown with alkalifeldspar and quartz; strongly pitted with voids and inclusions (hydrothermal ?)

Aegirine (7%) yellowish green, medium-grained anhedral, fractured and broken out of the section, intergrown with arfvedsonite

Arfvedsonite (20%) medium-grained anhedral, deep ink blue to olive-brown pleochroic mostly replaced by dark red-brown UM (aenigmatite?) and hematite

Monazite (1%) medium-grained, anhedral, colourless, high relief with blue-grey interference colour and pebbly surface texture, fractures (has some cleavage) intergrown with aegirine, feldspar, and quartz

Pyrochlore (trace) extremely fine-grained, clear to fine-grained, euhedral, olive-green, isotropic, trapezoidal crystals intergrown with aegirine-arfvedsonite, the smaller ones in quartz/feldspar

Fluorite (trace) fine-grained anhedral, rounded grains with abundant round inclusions, associated with quartz-feldspar and aegirine

Appendix B6 continued.

Sample 15-MPB-010A continued

Unknown Mineral UM8 (1%) very fine-grained, colloform, pale yellow to reddish brown aggregates in feldspar, partially replaced by hematite?

Unknown Mineral UM9 (trace) fine- to medium-grained, euhedral, blocky, high-relief mineral with very high interference colour (masked by pale yellow-green to pale orange absorption colour) intergrown with aefvedsonite

Hematite (1%) minor rusty to black staining and colloform aggregates in Fe-silicates (aegirine/arfvedsonite) and secondary Zr-minerals in voids

Microprobe analysis locations on polished thin section:

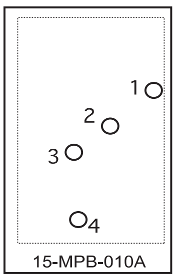

1) high-relief, colourless, anhedral mineral with low interference colour (anomalous blue-grey)

intergrown with quartz and feldspar, aegirine

2) high-relief, greenish, anhedral mineral (epidote-like) interstitial to feldspar

3) high-relief euhedral, pale green-orange mineral included in arfvedsonite-aenigmatite

4) aenigmatite in arfvedsonite intergrown with aegirine and UM9, pyrochlore, UM1, and hematite in quartz interstitial to feldspar